The last reconnection of the Marmara Sea (Turkey) to the World Ocean: A paleoceanographic and paleoclimatic perspective

by

*[1,2]Cecilia M. G. McHugh, [1]Damayanti Gurung, [3]Liviu Giosan, [2]William B. F. Ryan, [4]Yossi Mart, [5]Ummuhan Sancar, [2]Lloyd Burckle, [5]M. Namik Çagatay

[1] Queens College, The City University of New York, Flushing, NY, USA; [2]Lamont-Doherty Earth Observatory of Columbia University, Palisades, NY, USA; [3]Woods Hole Oceanographic Institution, Woods Hole, MA., USA;

[4]Recanati Institute for Marine Studies, University of Haifa, Haifa, Israel;

[5]Istanbul Technical University, Faculty of Mines, Ayazaga, Istanbul, Turkey

*Correspondent author

E-mail address: cmchugh@qc.cuny.edu; **cecilia@ldeo.columbia.edu**

Abstract

During the late glacial, marine isotope Stage 2, the Marmara Sea transformed into a brackish lake as global sea level fell below the sill in the Dardanelles Strait. A record of the basin's reconnection to the global ocean is preserved in its sediments permitting the extraction of the paleoceanographic and paleoclimatic history of the region. The goal of this study is to develop a high-resolution record of the lacustrine to marine transition of Marmara Sea in order to

reconstruct regional and global climatic events at a millennial scale. For this purpose, we mapped the paleoshorelines of Marmara Sea along the northern, eastern, and southern shelves at Çekmece, Prince Islands, and Imrali, using data from multibeam bathymetry, high-resolution subbottom profiling (chirp) and ten sediment cores. Detailed sedimentologic, biostratigraphic (foraminifers, mollusk, diatoms), X-ray fluorescence geochemical scanning, and oxygen and carbon stable isotope analyses correlated to a calibrated radiocarbon chronology provided evidence for cold and dry conditions prior to 15 ka BP, warm conditions of the Bolling-Allerod from ~15 to 13 ka BP, a rapid marine incursion at 12 ka BP, still stand of Marmara Sea and sediment reworking of the paleoshorelines during the Younger Dryas at ~11.5 to 10.5 ka BP, and development of strong stratification and influx of nutrients as Black Sea waters spilled into Marmara Sea at 9.2 ka BP. Stable environmental conditions developed in Marmara Sea after 6.0 ka BP as sea-level reached its present shoreline and the basin floors filled with sediments achieving their present configuration.

Key Words: late Pleistocene-Holocene; Marmara Sea; sea-level; paleoshorelines; Black Sea; Mediterranean Sea

Introduction

Reconnections of marginal basins to the World Ocean after the late glacial eustatic lowstand can help track global sea-level rise due to the amplified sedimentation changes and complete replacement in the fauna and flora that occurs when these basins switch from lacustrine to marine conditions. Intracontinental basins tend to be small and respond to environmental changes rapidly. Therefore such basins have the potential to capture high-resolution regional and global paleoclimatic and paleoceanographic variability in their sedimentary records (Leventer et al., 1982; Thunell and Williams, 1989; Peterson et al., 1991; Behl and Kennett, 1996; Hughen et al., 1996; Sidall et al., 2003; Ortiz et al., 2004; Major et al., 2006).

The Marmara Sea is an intracontinental basin 275 km long and 80 km wide formed as a result of pull-apart tectonics along the North Anatolia Fault (Fig. 1; Sengör et al., 1985; Görür et al., 1997; Armijo et al., 1999; 2002; 2005; Okay et al., 1999; Le Pichon et al., 2001; Demirbag et al., 2003). The geological evolution of the Marmara Sea began in the Neogene, late Serravallian, Miocene, and possibly as late as the Plio-Pleistocene. Marmara Sea is divided into three major sub-basins, named Tekirdag, Central, and Çinarcik, from west to east, that are ~ 1200 m deep. Saddles as shallow as 400 - 600 mbsl separate these basins (Fig. 1). The northern shelf of Marmara Sea is narrow (~15 km). In contrast, the southern shelf is as broad as 50 km. The dimensions of the drainage basins and river discharge are quite different on the northern and southern margins. To the north the drainage basin is 4,438 km^2 in extent, and there are only small streams with no significant discharge (Okay and Ergun, 2005). In contrast, the drainage to the southern margin extends over an area of 30,600 km^2 and drains several medium-sized rivers with a total sediment delivery of 6.3×10^6 tons/yr (Ergin et al., 1991).

70 The Marmara Sea is connected to the Aegean Sea through the Dardanelles Strait (Görür et
71 al., 1997; Çagatay et al., 1999; 2000). Recent studies by Gökasan et al. (2008) showed that the
72 Dardanelles Strait is 74 km long, 1.3 to 7.5 km wide with average water depths of -60 m. During
73 the last glacial when Marmara Lake was isolated from the Mediterranean Sea, water depths
74 along the Dardanelles Strait averaged -85 m (Gökasan et al., 2008). Marmara Sea is connected
75 to the Black Sea through the Bosporus Strait (Gökasan et al., 1997; 2005). The Strait is 31 km
76 long, and its width varies from 0.7 to 3.5 km (Algan et al., 2001; Gökasan et al., 1997; 2005).
77 Sills located at the southern and northern entrances of the Bosporus Strait are -35 m and -58 m
78 deep, respectively. The basement topography is irregular and characterized by sills of -120 m to
79 the south and -80 m to -70 m towards the north.
80 The oceanography of the Marmara Sea is characterized by the outflow of brackish water
81 from the Black Sea with salinity of 18‰ and inflow of saline intermediate and bottom water
82 (38‰) from the Aegean Sea (Besiktepe et al., 1994). Water and suspended sediments are
83 delivered to Marmara Sea from the Straits of Dardanelles and Bosporus. These straits help
84 maintain the balance between water supply and evaporation. The flux rate of suspended solids
85 for the Dardanelles Strait is 9.0×10^5 tons/yr and for the Bosporus Strait, 14.5×10^5 tons/yr (Ergin
86 et al., 1991). During the last glacial, marine isotope Stage 2, when global sea-level dropped
87 below the -85 m Dardanelles Sill, Marmara lost its connection from the global ocean and became
88 a fresh-brackish water lake (Stantley and Blanpied, 1980; Ryan et al., 1997; 2003; Aksu et al.,
89 1999; 2002; Çagatay et al., 1999; 2000). Although the reconnection of Marmara Sea to the
90 Mediterranean Sea has been previously documented, questions remain regarding the level of
91 Marmara Lake at the time of marine incursion and whether the Black Sea outflow to Marmara
92 was vigorous and continuous at the time of the reconnection (Ross and Degens, 1974; Stanley

93 and Blanpied, 1980; Lane-Serff et al., 1997; Aksu et al., 1999; 2002; Kaminsky et al., 2002;
94 Mudie et al., 2002) or discontinuous (Ryan et al., 1997; 2003; Major et al., 2002; 2006; Myers et
95 al., 2003; Sperling et al., 2003; Giosan et al., 2005). Due to its irregular basement topography
96 and sediment thicknesses, there are questions as to whether the depth of the Bosporus Strait was
97 shallow or deep during the reconnections. Some authors have concentrated on characterizing the
98 stratigraphy, sediment infill, delta formation, and physical oceanography to shed light into this
99 problem (Ergin et al., 1991; Algan et al., 2001; Hiscott et al., 2002; Myers et al., 2003; Sidall et
100 al., 2004; Gökasan et al., 1997; 2005; Eris et al., 2007).

101 This study uses geophysical, sedimentological, biostratigraphic, physical and geochemical
102 data, as well as stable isotopes obtained from foraminifera to document the reconnection of
103 Marmara Lake to the global ocean and to address the following questions. 1) Was the surface of
104 the Marmara Lake below its outlet to the Aegean Sea just prior to the reconnection? If so, was
105 this indicative of regional drought conditions? 2) Was the Marmara Lake isolated from the Black
106 Sea during its reconnection to the global ocean? 3) Was the incursion of marine waters in the
107 brackish-fresh water lake rapid and accompanied by extensive changes in paleo-depositional
108 environments (i.e., the migration of the shoreface and drowning of river beds), faunal (mollusks,
109 foraminifers) and floral (diatom) assemblages? 4) What paleoclimatic and paleoceanographic
110 events can be detected in the lake and marine records and can these events be recognized at
111 millennial-scale variability?

112 The data that forms the basis for this study was collected during geophysical surveys and
113 sediment sampling conducted from the *R/V Mediterranean Explorer* in the summer of 2005 (Fig.
114 1; Mart et al., 2006) and from the *R/V Urania* in 2001 (Çagatay et al., 2003; Polonia et al., 2004;
115 Cormier et al., 2006). We mapped the paleoshorelines of Marmara Lake along the northern,

116 eastern, and southern shelves at Çekmece, Prince Islands, and Imrali, respectively. Multibeam
117 bathymetry, high-resolution subbottom profiling (chirp) and sediment cores were obtained from
118 present water depths of -75 to -300 m.
119

120 **Methods**

121 The *R/V Mediterranean Explorer* geophysical survey was conducted with an Edgetech
122 SB424 chirp reflection profiler navigated by GPS. N-S and E-W track lines were separated at
123 0.1' spacing (185 - 150 meters). Each surveyed area was approximately 4 by 6 km wide. The
124 digital field data were sampled at a 0.125 millisecond interval across a 0.2 second window and
125 recorded in EdgeTech format. The files were converted to segy format for shipboard analysis
126 with the TKS Kingdom Suite® software package. Gravity coring was conducted with a 10 cm
127 diameter and up to 3 m long barrel with a 400 kg core head. The *R/V Mediterranean Explorer*
128 sediment cores were recovered from the Çekmece and Prince Islands margins. The cores were
129 split, photographed, described and sampled in the ship's laboratory. U-channels were taken from
130 each 1.5 m core section for bulk X-ray fluorescence (XRF) geochemical scanning conducted
131 every 1 mm along the sediment surface. Bromine relative content (in counts/second), as
132 measured by the XRF scanner, was used to estimate the presence of marine organic matter in the
133 sediments. Bromine is thought to be preferentially associated to marine rather than freshwater-
134 derived organic matter (Malcolm and Price, 1984). The calcium carbonate content of the
135 sediments was measured every 5 cm using a Coulometric carbonate-carbon analyzer. The
136 accuracy of this method was $\pm$0.05%. Carbonate content is expressed as wt% $CaCO_3$, assuming
137 that all the carbonate was present as calcite. Cores are archived (one half each) at the Istanbul
138 Technical University and the University of Haifa.

139 High-resolution multibeam (ELAC1180 system) and subbottom CHIRP profiling (hull
140 mounted Datasonics) conducted at 50 m spaced grids, were obtained from the *R/V Urania* in the
141 summer of 2001 (Çagatay et al., 2003; Polonia et al., 2002; 2004; Cormier et al., 2006). Precise
142 navigation was provided by differential GPS positioning and bathymetric maps are referenced to
143 the WGS84 datum. The physical properties of the cores were measured on board of the *R/V*
144 *Urania* with a Geotech core logger (Polonia et al., 2002). The studied gravity cores IM03 and
145 IM05 were recovered from the Imrali margin from the *R/V Urania*. To recover the water and
146 undisturbed underlying sediment, the SW-104 coring system was used.
147 Oxygen isotopes were conducted at the Woods Hole Micropaleontology Mass Spectrometer
148 Facility with a Finnegan MAT253 mass spectrometer from the tests of the benthic marine
149 foraminifer *Brizalina spp*. A chronology was established from ^{14}C derived from mollusks and
150 foraminifers (Table 1). Radiocarbon dating was conducted at the NOSAMS Facility at Woods
151 Hole, MA. Given the great variability in water masses of the Marmara Sea ages are reported as
152 both calibrated years BP and radiocarbon years BP (Table 1). Calibrated ages were obtained by
153 applying Sinai et al. (2000) reservoir correction. The ages were converted to calendar years with
154 CALIB 5.0 program (Stuvier and Reimer, 1993). All the cores identification, water depth and
155 coordinates are described in Table 2 in the Supplementary Data.
156 All sediment cores were sampled every 5 cm for foraminiferal and mollusk biostratigraphy,
157 except for Cores IM03 and Core 8 that were sampled every 10 cm (Gurung et al., 2006). All the
158 samples were wet sieved through a 63 μm sieve and the fractions of the sample > 63 μm were
159 dried and picked for analyses. Mollusks were identified to genus level using Abbott and Dance
160 (1990) and Vaught et al. (1989) and 22 genera were identified. The dominant taxa that were
161 considered before the marine incursion are fresh-brackish mollusks of Caspian affinity and

characteristic of Neoeuxinian Black Sea sediments *Dreissena* sp. and *Theodoxus* sp. (Fedorov, 1971; Ross and Degens, 1974). After the marine intrusion the molluskan fauna is indicated by shallow littoral marine species of Mediterranean affinity *Gouldia sp., Lucinella sp., Corbula sp., Cardium sp*. (Tables 3-11 in Supplementary Data). Foraminifers, at least 300, were picked from 10 g sub-samples, identified to genus level with a binocular microscope, counted, and standardized by calculating percent abundance within each sample (Tables 12-21 in Supplementary Data). Benthic foraminiferal species were identified and counted for Core IM05, and Mediterranean Explorer Cores 6, and 1 on the southern (Imrali), northern (Çekmece), and Prince Islands margins of Marmara Sea (Taxonomy in Appendix A). These cores were chosen to identify species because of their continuous sedimentation as documented by the lithostratigraphy and radiocarbon chronology. Foraminiferal taxonomy is based on Loeblich and Tappan (1988). Further identification to genera and species level was carried out by using Phleger (1960), Murray (1971; 1986), Haynes (1981), Yanko and Troitskaja (1987), Alavi (1988), Cimmerman and Langer (1991), Sgarella and Moncharmont Zei (1993), Lee et al. (2000), Kaminski et al. (2002), Hayward et al. (2003), and Meric et al. (2004).

Samples for diatom studies were taken every 5 cm in Core IM05 and every 10 cm for Core IM03, chemically treated with 10% hydrogen peroxide and 10% hydrochloric acid to extract the diatoms, and thin sections were prepared without heating the samples. The method used represents a slight modification from Renberg (1990). Two hundred diatom valves were counted from each interval, identified to the genus level using Round et al. (1990) and grouped into: freshwater, brackish, and marine (Table 22 in Supplementary Data). Fresh and brackish water diatoms are better preserved in the sediments because they have thick-walls. In contrast marine diatoms are thinner walled, more susceptible to dissolution and not well preserved. The absence

of all diatoms in the sediments that contain marine foraminiferal and mollusk assemblages is interpreted as the result of dissolution rather than low productivity.

Results

Southern Shelf at Imrali

The Imrali shelf-slope region along the Southern Boundary Fault was surveyed between -80 m and -300 m of water depth (Fig. 2). The goal of the survey was to document neotectonic activity along the Southern Boundary Fault and to map the paleoshorelines. The topography of the surveyed region, has a steep slope (up to 20°) that subbottom profile records show was created by normal fault activity and a series of rotational slumps concave to the basin (McHugh et al., 2006; Fig. 2). A transect of cores was obtained extending from present water depths of -100 to -300 m. Cores IM05 was recovered from 152 m of water depth at the base of one of these scarps. After reconstruction of the 30 m of vertical offset during the Holocene (past 10,000 yrs) due to faulting and slumping processes, Core IM05 was positioned at -115 m of present water depth (McHugh et al., 2006; Fig. 3). The reconstruction was based on the identification of the seismic reflector that represents the lacustrine to marine transition from the lithology, biostratigraphy and radiocarbon dating. The vertical offsets were measured from the seismic lines and the seismic reflector reconstructed to its original position. Core IM03 was taken at -298 m of water depth, 1 km away from the fault, and its sediments were not offset by fault activity. Three terraces were delineated from the reconstructed subbottom profiles at -87 m, -95 m, and -115 m of water depth (Fig. 3).

Sediments, flora, mollusks

208 Core IM05 was subdivided into four sedimentary facies based on its texture, flora, and
209 fauna (Fig. 4). Facies 1: lacustrine-barren is composed of laminated silty clays with abundant
210 woody material and rare fragments of Neoeuxinian-Caspian affinity mollusks of *Dreissena*
211 *rostriformis* and the gastropod *Theodoxus fluviatilis* (Fedorov, 1971; Ross and Degens, 1974).
212 Sediments of Facies 1 are older than 15.0 ka BP (13.15 ^{14}C ka BP). Facies 2: lacustrine-fertile is
213 composed of silty clays with abundant mollusks dominated by *Dreissena* sp. banks and also by
214 the gastropod *T. fluviatilis*. These two assemblages were typical of brackish water environments
215 with salinities of 1-5‰. The lake sediments of Facies 2 also contain brackish water diatoms
216 *Cyclotella spp; Cocconeis spp; Diploneis spp.* and *Amphora spp* and freshwater diatoms
217 *Stephanodiscus spp; Fragilaria spp; Eunotia spp; Navicula spp; Cymbella spp; Cystopleura spp.*
218 During the lake-fertile stage sedimentation rates were as high as 0.4 cm/year (Fig. 5). Sediments
219 of Facies 2 were deposited between 15.0 to 12.0 ka BP (13.15 ^{14}C ka BP and 11.0 ^{14}C ka BP;
220 Table 1). Facies 3 represents the marine incursion surface and is composed of a 20 cm-thick
221 gravelly sand bed containing flat pebbles typical of a beach environment. A marine mollusk
222 above the sand bed was dated at 11.8 ka BP (10.7 ^{14}C ka BP). Facies 3 separates lacustrine from
223 marine strata and marks a major transformation in the sediments, flora and fauna. Facies 4 is
224 entirely composed of marine sediments and fauna. The sediments are clayey silts and contain
225 marine mollusks, marine benthic and planktonic foraminiferal assemblages. Marine diatom tests
226 were rarely preserved in the sedimentary record due to their dissolution in the water column.
227 Sediments of Facies 4 were deposited from 11.83 ka BP (10.7 ^{14}C ka BP) to the present.
228 Sedimentation rates for the marine facies were very stable at 0.02 cm/yr (Fig. 5). Core IM03 is
229 composed of marine muds and marine fauna and it is 350 cm long. No diatoms were found in
230 Core IM03. The lower section of Core IM03 is laminated and the sparse occurrence of benthic

231 and planktonic foraminifers suggests that its base was very close to the lake sediments. Core
232 IM03 was dated at 5.7 ka BP (5.4 ^{14}C ka BP) at 230 cm and 5.5 ka BP (5.3 ^{14}C ka BP) at 150 cm
233 and correlated to Core IM05 based on the radiocarbon ages (Table 1).
234
235 ***Physical Properties***
236 The bulk density, p-wave velocity and magnetic susceptibility of the sediments were
237 measured on cores IM05 and IM03. They showed an abrupt change at the contact between the
238 lacustrine and marine facies (Fig. 6). The bulk density measurements increased upwards in the
239 core from 1.9 g/cm^3 in the lacustrine-barren Facies 1 to 2.3 g/ cm^3 in the lacustrine-fertile Facies
240 2. These high values of bulk density in the lacustrine facies are indicative of low pore water
241 content. In the upper marine part of the core (Facies 4) bulk densities decrease further to values
242 of 1.55 g/ cm^3 that are typical of water-saturated surface sediments. The abrupt contact between
243 the lacustrine and marine facies is also accompanied by a decrease in the P-wave velocity from
244 1650m/s to 1550m/s. The magnetic susceptibility values also exhibited changes from the
245 lacustrine to the marine facies with highest susceptibility at 25 cm and 140 cm below the contact.
246
247 ***Benthic and Planktonic Foraminifers***
248 All shelf-slope cores from the southern Marmara margin at Imrali and northern margin at
249 Prince Islands and Çekmece contain similar benthic foraminiferal assemblages (Fig. 7; Gurung et
250 al., 2006). The record of benthic foraminifers in the outer shelf was appropriate for
251 environmental analyses because benthic foraminifers respond rapidly to changing conditions
252 such as deepening, sediment supply, organic matter, and oxygen concentrations (Sen Gupta et
253 al., 1993; 1996). For this study we classified benthic foraminifers based on Murray (1991, 2006),

254 Kaiko (1994), Cannariato et al. (1999), Kaminski et al. (2002) and Meric and Algan (2007) into
255 two major subgroups: 1) low oxygen concentrations or suboxic: *Brizalina spp., Bulimina spp.,*
256 and *Cassidulina spp*., and 2) shallow water, tolerant of a wide range in salinity: *Elphidium spp*.
257 and *Ammonia spp*. Some species such as *Hyalinea spp*. and *Globobulimina spp*. reflect the
258 development of water stratification and high organic carbon flux in shelf environments and have
259 been used to interpret these environmental conditions (Murray 1991, 2006; Schonfeld, 1997;
260 2001; den Dulk et al., 2000; Evans et al., 2002; Fontanier et al., 2002, 2003).

261 Twenty benthic foraminiferal species were found in Core IM05 that indicate changes of
262 salinity, water depth, deepening and development of stratification in the water column. Benthic
263 foraminiferal assemblages were first established during the initial incursion of marine waters at
264 around 12.0 ka BP (10.7 ^{14}C ka BP). From 12 ka BP to 11.0 ka BP *Cassidulina carinata* and then
265 *Brizalina spp*. (*B. catanensis, B. spathulata*) were the first marine foraminifers present in the
266 sedimentary record of IM05. Except for the initial marine incursion in which only two species
267 were dominant *Brizalina spp*. (*B. catanensis, B. spathulata*, *B. alata, B. striatula)* exhibited
268 similar patterns throughout the core and has been grouped by genus. The species *Ammonia*
269 *tepida*, *E. macellum,* and *E. articulatum* were also present during the initial marine incursion,
270 from 12 ka BP to 11.0 ka BP, and they indicate that the sediments were deposited in a shallow
271 water environment with a wide range in salinity conditions (Debenay et al., 1998; Murray, 2006;
272 Meric and Algan, 2007; Fig. 7). *E. macellum* is characteristic of seagrass, marsh assemblages
273 further suggesting nearshore environment (Murray, 1991).

274 The relative abundances of *C. carinata*. and *Brizalina spp*. decreased from 11.5 ka BP to 10.0
275 ka BP and benthic foraminiferal species were dominated by *Bulimina aculeate*. *Bulimina spp. (B.*
276 *aculeate; B. costata; B. marginata; B. elongata)* behaved in a similar patter throughout the rest

277 of the core and was grouped by genus. Deepening was manifested by the near disappearance of
278 the shallow water species *Elphidium spp*. and *A. tepida* and by the appearance of planktonic
279 foraminifers at ~11.0 ka BP. *Hyalinea balthica* made its first appearance at ~11.0 ka BP. *H.*
280 *balthica* has been interpreted as an indicator for the onset of stratification in the water column in
281 other shelf settings (Scourse et al., 2002; Evans et al., 2002; Murray 2006). Large increases of
282 specimens of *H. balthica* occurred at 9.1 ka BP and ~6.0 ka BP and they are interpreted as
283 having been produced by outflow of Black Sea waters, and due to deepening as sea level reached
284 near its present position, respectively. *Globobulimina affinis* is associated to high organic flux
285 (>3.5 g C m^{-2} per year) tolerates dysoxia but can also be found under oxic conditions (Schonfeld,
286 1997, 2001; den Dulk et al., 2000; Fontanier et al., 2002, 2003; Murray 2006). Large increases in
287 the abundance of *G. affinis* at ~10 ka BP, 9.1 ka BP and 8.0 ka BP are interpreted as influx of
288 nutrients after the Younger Dryas, and outflow of Black Sea waters. After ~6.0 ka BP all benthic
289 foraminifers showed little variability except for the appearance of *A. beccarii* a much more
290 tolerant form of *Ammonia spp*. (Fig. 7; Thomas et al., 2000). The relative abundances of
291 planktonic foraminifers decreased from 35% to 15% after 3.24 ka BP (Fig. 7).
292

293 ***Stable Isotopes***

294 The oxygen isotope record of cores IM05 and IM03 recovered at -150 and -300 m of water
295 depth, respectively, showed values ranging from 2.2 ‰ $\delta^{18}O$ at ~12.0 ka BP to 1.5 ‰ $\delta^{18}O$ at
296 present (Fig. 8a). Both cores showed a trend from heavy to light values that reflect high salinity
297 and colder temperatures during the initial incursion of marine waters. The waters gradually
298 freshened and warmed throughout the Holocene.

299 Carbon isotopes ranged from -2.5 to -0.5 ‰ $\delta^{13}C$ showing an overall trend to less depleted
300 values. This could be related to a decrease in the organic matter flux and rates of sedimentation
301 as Marmara Sea deepened and the shoreline approached its present position. The $\delta^{13}C$ values of
302 IM05 and IM03 can be correlated in the upper meter of both cores from ~5.0 ka BP to the
303 present, indicating that environmental conditions remained stable at both locations within the
304 past 5.0 ka (Fig. 8b).
305
306 ***Eastern Shelf at Prince Islands***
307 The Prince Islands shelf was surveyed from -80 to -120 m of water depth (Fig. 9). The
308 subbottom profile records showed a terrace at -93 m of water depth, deeper than the -85 m lake
309 paleoshoreline, and of comparable depth to the paleoshoreline on the Imrali margin. Four cores
310 were recovered from the shelf-slope boundary Core 7 at -88 m, Core 5 at -92 m, Core 6 at -98 m,
311 and Core 8 at -109 m (Table 1 in Supplementary Data; Fig. 9). The coring strategy was based on
312 the expectation of reaching older strata that may have been truncated by erosion during the lake
313 stage of Marmara for reconstructing the lacustrine to marine transition. The oldest sediments
314 were expected to be at the shallowest depths where sub-aerial exposure of the shelf would have
315 led to more erosion. The youngest sediments were expected to be at the deepest parts of the study
316 area due to sediment progradation of younger strata over old, and to the generally better
317 preservation of deeper strata. Cores 6-8 recovered marine sediments and Core 5 penetrated
318 lacustrine strata (Figs. 10-11; Gurung et al., 2006). When compared to lacustrine values (Fig.
319 12), high Br content of over ~200 counts/sec also indicated the presence of marine rather than
320 fresh water-derived organic matter in the cores recovered in this region. Core 5 was dated at 10.7
321 ka BP (9.9 ^{14}C ka BP) at 70 cm and 11.5 ka BP (10.4 ^{14}C ka BP) at 80 cm. An age of 12.0 ka BP

was estimated at 100 cm (Fig. 10). The base of Core 6 was dated from a marine mollusk at 11.7 ka BP (10.6 ^{14}C ka BP). Core 7 was very short (60 cm). We attributed this lack of penetration and sediment recovery to the stiffness of the low-water content lacustrine strata. The low water content and high bulk density of the lacustrine substrate at or shallower than the present substrate at the -87.5 m isobath was most likely intermittently exposed when the Marmara Lake reached its low stand prior to 12 ka BP.

Sediments, mollusks

All four cores (5-8) were primarily composed of silty clay with sandy mud/muddy sand in the lower 30 cm (Fig. 10). Only Core 5 contained solely lacustrine mollusks at its base. All other cores contained reworked mollusk shells of both marine and fresh water affinity i.e., *Corbula spp*. and *Dreissena spp*., respectively, at the bottom suggestive that the marine-lacustrine transition was close but not recovered. Also present towards the base of the cores were charcoal fragments, medium-grained, very well-sorted, and very well-rounded, black sands interbedded with intervals of very indurated clays. Note that very indurated lithologies were also recovered in the lacustrine facies of Imrali and are present at or immediately above the lacustrine-marine transition suggestive of exposure of the shelf. The calcium carbonate measured in the sediments ranges from 10 to 40% and it reached its greatest weight percent near or at the marine-lacustrine transition (Fig. 13).

Benthic and Planktonic Foraminifers

Following the submersion of the shelf edges at ~12 ka BP, *C. carinata* was the first abundant marine benthic foraminifer to appear in the sedimentary succession (Fig. 11). The

occurrence of marsh and shallow water *A. tepida a*nd *Elphidium spp.* (*E. crispum, E. articulatum, E. macellum*) at 11.75 ka BP (10.6 ^{14}C ka BP) in Core 6 and 11.5 ka BP (10.5 ^{14}C ka BP) in Core 5, document the initial marine transgression. From 11.75 to 10.0 ka BP (10.6 to 9.3 ^{14}C ka BP) *C. carinata* is replaced first by *Brizalina spp.* (*B. catanensis, B. spathulata*) and then by *Bulimina spp.* dominated by *B. aculeata* (Fig. 11). After 10 ky BP *A. tepida* and *Elphidium spp.* disappear as the shelf further submerges. Planktonic foraminifers appear in abundance. A very unusual 50 cm thick deposit was found from 100 to 150 cm in Core 6 (Fig. 10). The sediments within this interval consist of homogeneous silty clays and contain fragments of marine mollusks and foraminifers. On the chirp records the deposit appears as a 2 m thick semi-transparent unit interpreted as a homogenite. Earthquakes have been linked to such deposits in the Marmara Sea. The strong shaking of slope sediments generated by an earthquake and seismically induced turbidity currents lead to the resuspension, dilution, and redeposition of fine-grained sediment the settles to the sea floor draping the basin and forming homogenous deposits (McHugh et al., 2006). A similar process where sediment was stirred and remained in suspension for several months and produced a homogeneous deposit was documented after the 1997 Cariaco Basin earthquake and the 1994 Sanriku-Oki earthquake (Thunell et al., 1999; Itou et al., 2000). After 6 ka BP the suboxic *C. carinata*, *Brizalina spp.* and *Bulimina spp.* remain stable in their relative abundances.

Northern Shelf at Çekmece

The northern shelf of Marmara Sea at Çekmece was characterized by occurrences of three terraces located at -87 m, -93 m and -102 m of water depth (Fig. 14). Cores 4, 1, 2, and 3 were recovered from -118 m, -102 m, -93.3 m, and -93m respectively. The limited penetration for

Cores 3 and 4 suggests that they bottom a similar stiff, low-water content lacustrine facies as recovered in the IM05 core (Fig. 14). However, the mollusks *Dreissena sp*. and *Theodoxus sp*. reveal that lacustrine sediments were reached and recovered in limited thicknesses in Cores 1 and 2. The marine incursion was dated at 11.5 ka BP some 14 cm above the top of lacustrine sediments providing a minimum age for the event (Fig. 15). Lacustrine sediments were composed of clayey silts with abundant black stains and charcoal fragments. Low Br content (<200 counts/sec) indicates that organic matter is not of marine origin in these sediments (Fig. 12). Unfossiliferous beds of indurated clays separated the lacustrine and marine sediments. The marine sediments in all cores are composed primarily of silty clays and sandy muds interrupted by occasional reworked intervals manifested by the mixed mollusk assemblages (marine, lacustrine) and by the ages that showed old above young (Cores 1 and 3; Fig. 14). The transition from lacustrine to marine sediments is characterized by a high variability in Br content that may be indicative of a variable marine-freshwater character of the basin, but more likely reflecting reworking and redeposition of sediments in the region (Fig. 12). Calcium carbonate weight percentage is greatest (up to 40 wt%) within the lacustrine sediments and close to the lacustrine-marine transition but decreases up core (Fig. 13).

Benthic and Planktonic Foraminifers

Benthic foraminiferal assemblages showed very similar patterns as those from Imrali and Prince Islands (Fig. 16). *A. tepida* is present towards the base of the core with a prominent abundance peak at ~11.5 ka BP in Core 1 (-102 m). The abundance of *Elphidium spp*. decreases up core. *Bulimina spp*. and *Brizalina spp*. are dominated by *B. aculeata* and *B. spathulata*, respectively. From approximately 11.5 to 9.4 ka BP, *H. balthica* and *G. affinis* show peak

391 abundances similar to those documented in the Imrali margin and interpreted as water
392 stratification and nutrient influx possibly due to the Younger Dryas and Black Sea outflow. The
393 part of the sedimentary record extending from 7.35 ka BP (6.9 ^{14}C ka BP) to the present showed
394 a stable abundance of suboxic foraminifers with *Brizalina spp*. dominating the assemblages.
395
396
397 **Discussion**
398
399 The Marmara Sea has captured in its sediments, fauna and flora, paleoclimatic and
400 paleoceanographic changes for approximately the past 15 ka BP (13.0 ^{14}C ka BP), at thousand-
401 year scales, demonstrating how marginal basins are sensitive to changing paleoenvironmental
402 conditions. The different proxies used (lithology, benthic and planktonic foraminifers, mollusk
403 assemblages, diatoms, physical and geochemical properties and stable isotopes) permitted to
404 track global sea level as it breached the Dardanelles and Bosporus sills and reached its present
405 position allowing for the Mediterranean, Marmara, and Black Sea waters to establish the present
406 day circulation. The measured data allowed us to reconstruct a sequence of events described
407 below (Fig. 17). The ages are listed as calibrated years for global comparison.
408
409 ***Marmara Lacustrine Stage (>15.5 ka BP to 12.0 ka BP)***
410 The deglaciation of the Eurasia continental ice was initiated at 18.0 ka BP and extended
411 until 15.8 ka BP (Bard et al., 1990; Grosswald 1980; 1998; Denton et al., 1999; Svitoch, 1999;
412 Bahr et al., 2005). The effects of the Eurasia deglaciation can be expanded to the Black-Marmara
413 Sea corridor until ~15.5 ka BP through a Caspian-Black Sea connection (Bahr et al., 2005). Once

414 the initial disintegration of the Eurasian continental ice occurred, the retreating ice was not
415 longer a source of meltwater to the Black Sea and consequently for the Marmara Lake (Bahr et
416 al., 2005; Major et al., 2006). The oldest sediments recovered provide evidence of Marmara Lake
417 isolated from the global ocean. The Lake sediments were laminated, indicative of cyclic
418 sedimentation and oxic conditions (Fig. 4). Rivers were proximal bringing terrigenous sediment
419 and the abundant charcoal suggested that the climate was dry with possible fires (Figs. 4, 15).
420 The lake was nearly barren of fauna containing few *Dreissena sp*. and *Theodoxus sp*. of brackish
421 and freshwater affinity, and rare brackish and fresh water diatom flora. The magnetic
422 susceptibility data exhibits the greatest values during this barren lake stage. This signal is
423 interpreted as derived from terrigenous sediments transported by rivers that drained into a
424 proximal paleoshoreline (Fig. 6). Dry and cold climatic conditions and a sparsely vegetated
425 landscape, which facilitated the erosion and transport of sediment by rivers, were documented
426 for the Marmara and Black Sea regions at this time, except for the Black Sea southern coast,
427 based on pollen stratigraphy (Caner and Algan, 2002; Filipova-Marinova et al., 2004; Mudie et
428 al., 2001; 2007). From ~ 15.5 ka BP to 14.5 ka BP there is evidence for an abundant supply of
429 fresh water from the Black Sea (a lake at this time) into Marmara Lake. The lake paleoshorelines
430 lay at the level of its Dardanelles spillway to the Aegean Sea at -85 m, but isolated from the
431 world's oceans (Lane-Serff et al., 1997; Çagatay et al., 2000; Algan et al., 2001; Aksu et al.,
432 2002; Hiscott et al., 2002; Gökasan et al., 2008; Figs. 1, 17). Oligohaline conditions with
433 salinities of 1-5 ‰ were present as documented by the Caspian-like mollusk assemblages (Fig.
434 4*). Dreissena rostriformis* and *Theodoxus fluviatilis* were abundant. The $^{87}Sr/^{86}Sr$ compositions
435 of these mollusks have a Black Sea signature (Major personal communication 2006; Major et al.,
436 2006). The Bolling-Allerod interstadial brought warm conditions to Marmara Lake as manifested

by the sediments, fauna, and flora of the lacustrine facies. Brackish and freshwater diatoms and woody material became less abundant just prior to the marine incursion when the magnetic susceptibility is high relative to marine values (Fig. 6).

Marine Incursion - 12 ka BP

The incursion of Mediterranean waters, at ~12.0 ka BP was accompanied by the replacement of the fauna and flora, the introduction of marine derived organic matter as manifested by Br cts/s, and a decrease in grain size and calcium carbonate abundance (Figs. 4-7, 12). All these changes were abrupt as measured by the thickness of the sediment over which the change occurred. This thickness is typically a few centimeters. It indicates that a transitional stage, if present was brief. The abruptness in the cores from both the northern and southern shelves contradicts the calculations of Myers et al. (2003) based on hydraulic theory which predicts a transition as long as 2.7 ka.

Paleoshorelines have been studied in Marmara Lake and used to reconstruct the geologic and climatic history of the region (Ergin et al., 1997; Çagatay et al. 1999; 2000; 2003). The -85 m terrace has been documented as the lake paleoshoreline at the level of its Dardanelles spillway with the Mediterranean Sea and the -65 m terrace as evidence for the Younger Dryas stillstand. The -95 m terrace documented in this study marks an erosional surface that can be traced nearly continuously throughout the Marmara Sea (Imrali, Prince Islands and Çekmece margins). The -95 m terrace, first documented by Aksu et al., 1999, lies almost 10 m below the Dardanelles bedrock sill. This raises the possibility that the levels of the lake dropped momentarily below the sill before the Mediterranean waters spilled into Marmara, or that wave action in the lake beveled the lake floor to form a terrace 10 m below the lake surface. The Bolling Allerod, prior to 12 ka

460 BP, was warm and hence evaporation rates were perhaps high enough to draw down the lake
461 below its outlet. According to Major et al., (2006), the Black Sea responded similarly, expanding
462 when cool and shrinking when warm.

463 Evaporative conditions of Marmara Lake and early Marmara Sea could explain salinity
464 values of 4‰ greater than modern values calculated from alkenone measurements by Sperling et
465 al. (2003). The earliest marine sediments have the heaviest oxygen isotope signal (2.3‰ $\delta^{18}O$;
466 Fig. 8). An evaporative drawdown of the lake and subaerial exposure of the shelf edge would
467 leave a stiff and low water content substrate sampled at a depth below the Dardanelles spillway.

468 Authigenic carbonate precipitation is a common process in lakes experiencing evaporation.
469 High autigenic carbonate is abundant in the Black Sea terminal lacustrine succession (Bahr et al.,
470 2005; Major et al., 2006). In the deeper and permanently submerged regions of the Marmara Sea
471 an authigenic carbonate layer was dated at ~12.5-14.5 ka BP (11.3-13.0 ^{14}C ka BP; Reichel and
472 Halbach, 2007). Gypsum crystals were first reported by Stanley and Blanpied (1987) in the
473 sediments of this age. The shelf muds we measured of the same age contain up to 40% carbonate
474 (Fig. 13). Further work is needed to distinguish autigenic carbonate from the calcite of mollusk
475 shells.

476

477 ***Younger Dryas 11.5 – 10.5 ka BP***

478 The global transition from glacial to interglacial was interrupted by the Younger Dryas cold
479 interstadial (Mangerud et al., 1974; Fairbanks 1989). Our data indicates that the Younger Dryas
480 occurred in the Marmara Sea soon after the marine incursion. A fresh water outflow from the
481 Black Sea into Marmara Sea could have been active during the Younger Dryas as proposed by
482 Major et al. (2002) but there is uncertainty as to weather it was vigorous (Çagatay et al., 2000;

483 Algan et al., 2001; Aksu et al., 2002; Hiscott et al., 2002; Major et al., 2002; Eris et al., 2007), or
484 weak (Myers et al., 2003; Major et al., 2006). There is evidence of scour on the shelf at this time
485 because we occasionally find older shells above younger shells, all in the age range of 11.5 to
486 10.5 ka BP. There is evidence that the -65 m terrace in the Izmit Gulf was formed during a
487 Younger Dryas (Çagatay et al., 2003; Newman 2003). A still stand of sea level was likely during
488 the Younger Dryas, previously identified as the most arid period of the Last Glacial Age for the
489 Eastern Mediterranean and the near East based on pollen data (Rossignol-Strick, 1995; Filipova-
490 Marinova et al., 2004; Mudie et al., 2007).
491
492 ***Black Sea and Marmara Sea mixing of waters 9.4 – 9.2 ka BP***
493 The timing and mode of reconnection between the Mediterranean, Marmara, and Black Sea
494 has been heavily contested. Some studies proposed a non-catastrophic and gradual connection
495 between the Mediterranean-Black Sea corridor (i.e., Aksu et al., 2002; Hiscott et al., 2002; 2006)
496 while others proposed an abrupt and rapid process (i.e., Ryan et al., 1997, 2003; Major et al.,
497 2002, 2006; Myers et al., 2003; Sidall et al., 2004; Giosan et al., 2005). The detailed analyses of
498 benthic and planktonic foraminiferal assemblages from Marmara Sea shelves have provided
499 additional insights into how the Black Sea connection occurred. It is well established that
500 modern and ancient continental shelf waters undergo changes from oxic to anoxic conditions due
501 to seasonal fluctuations in temperature and salinity, and as a result of longer-term climatic
502 variability (Tyson and Pearson, 1991). Due to their rapid response, benthic foraminifers can
503 document these ecological changes (Tyson and Pearson, 1991; Sen Gupta et al., 1993; 1996;
504 Kaiho, 1994; Kaminski et al., 2002). Global sea level curves show that from 9.0 to 6.6 ka BP
505 sea-level was -50 to -15 m below present (Fairbanks, 1989). This means that the shelf edges were

506 sufficiently submerged to be able to experience variations in ventilation (Figs. 7, 11, 16).
507 Increases in the occurrence of benthic foraminifers *H. balthica* and *G. affinis* were recorded as
508 pulses in which their abundance increased from 0 to 30% (Figs. 7, 16). We interpret these pulses
509 beginning at 9.2 ka BP as a manifestation of water stratification and high nutrients due to Black
510 Sea outflow and the establishment of a two-layer circulation (Schonfeld, 1997, 2001; Dulk et al.,
511 2000; Evans et al., 2002; Fontanier et al., 2002, 2003; Murray 2006; Major et al., 2006). Later
512 pulses in the abundance of *H. balthica* and *G. affinis* at ~7.6 and 6.6 ka BP can be explained as
513 changes in organic matter flux that influenced biotic competition with resulting dominance of
514 one fauna over another (Fig. 7).
515
516 ***Sea-level reaching the present shoreline – 6 ka BP***
517 The stable environmental conditions that developed as sea level reached close to its present
518 position at 6.0 ka BP were manifested by the lack of change in the abundance of both benthic
519 and planktonic foraminiferal assemblages, the oxygen and carbon isotope records, and the
520 physical properties of the sediments (Figs. 6-8, 11, 16). A two layer circulation was well
521 established by this time with *Brizalina spp*. dominating the low oxygen concentration forms.
522 There were no major changes in water stratification and flux of organic mater as manifested by
523 the lack of variability in *H. balthica* and *G. affinis*. Only the highly adaptable *A. beccarii*
524 appears during this time. This species is known to be an opportunistic in other settings (Thomas
525 et al., 2000). Sedimentation continued in the Marmara Sea at a steady rate of 0.02 cm/year (Fig.
526 5). A slight decrease in the abundance of planktonic foraminiferal assemblages was observed at
527 the Imrali, Çekmece, and Prince Islands shelves (Figs. 7, 11, 16). The decrease can be linked to a
528 slight increase in the magnetic susceptibility of the sediments in Imrali, which may represent an

increase in magnetic minerals due to terrigenous transport (Figs. 6). Increased sediment supply due to deforestation in the Bronze Age is a possible explanation for the decrease in the biogenic proportion of the sediment (Eris et al., 2007).

Conclusions

The Marmara Sea is a small intracontinental basin that recorded in its sediments fluctuations in climate and water exchange between the Mediterranean and Black Seas demonstrating that such settings can serve as high-resolution repositories of environmental change. Our cores captured the pre-12 ka BP lacustrine lowstand, the onset of the marine incursion and the subsequent Holocene transgression. The Younger Dryas cold interstadial left a faunal signal and evidence of scouring and sediment reworking. The sediments and fauna record the Black Sea outflow beginning at 9.2 ka BP and the subsequent water column stratification as Marmara Sea established its two-layer circulation.

Acknowledgements

We are grateful to Andreas Weill and Eco-Ocean Association of Herzlyia, Israel for making the *R/V Mediterranean Explorer* survey possible. We also thank the Captain and crew of the *R/V Mediterranean Explorer* and *R/V Urania* for their expertise in the collection of the data. We are grateful to the Scientific Party of the *R/V Urania* and to Drs. Vachtman, Eris, Ulug and Sarikavak for their help during the expeditions. We thank Corinne Hartin and Dr. Karen Kohfeld for their help with analyses at Queens College. We thank Dr. Mustapha Ergin and an anonymous

reviewer for their comments that helped to improve the manuscript. Support for the analyses was from NSF-OCE-0222139; OCE-9807266 and PSC-CUNY 69138-00 38. This is a Lamont-Doherty Earth Observatory publication number ###.

Appendix A

The key species are listed in alphabetical order. The identification of the benthic foraminifera are carried out on the studies by Murray (1971), Yanko and Troitskaja (1987), Alavi (1988), Loeblich and Tappan (1988), Cimerman and Langer (1991), Sgarrella and Moncharmont Zei (1993), Kaminski et al (2002), Hayward et al. (2003), and Meric et al. (2004).

***Adelosina cliarensis* (Heron-Allen & Earland, 1930)**

1930 *Quinueloculina cliarenesis* Heron-Allen & Earland (p. 58, pl. 3, figs. 26, 31)

1991 *Adelosina cliarensis* (Heron-Allen & Earland) Cimerman and Langer (p. 26, pl. 18, figs. 1-4)

***Ammonia compacta* (Hofker, 1969)**

1969 Streblus compactus Hofker (p. 99, figs. 242-243)

1987 *Ammonia compacta* (Hofker), Yanko and Troitskaja (p. 44, pl. 11, figs. 1–10)

2002 *Ammonia compacta* (Hofker), Kaminski et al (pl. 5, fig. 8)

***Ammonia beccari* (Linné, 1758)**

1758 *Nautilus beccarii* Linné, (p. 710, pl. 1, fig. 1a-c)

1971 *Ammonia beccari* (Linné) Murray (p. 151, pl. 62, figs. 1-7)

***Ammonia tepida* (Cushman, 1926)**

1926 *Rotalia beccarii* (Linné) var. *tepida* Cushman (1926, p. 79, pl. 1)

1991 *Ammonia tepida* (Cushman) Cimerman and Langer (p. 76, pl. 87, figs. 10–12)

2003 *Ammonia tepida* (Cushman) Hayward et al (pl. 1, figs. 1-3)

***Asterigerinata mamilla* (Williamson, 1858)**

1858 *Rosalina mamilla* Williamson (p. 54, pl. 4, figs. 109–111)

1971 *Asterigerinata mamilla* (Williamson) Murray (1971, p. 141, pl. 59, figs. 1-9)

1991 *Asterigerinata mamilla* (Williamson) Cimerman and Langer (p. 73, pl. 82, figs. 1–4)

***Bigenerina nodosaria* d'Orbigny, 1826**

1826 *Bigenerina nodosaria* d'Orbigny (p. 261, pl. 11, figs. 9-12)

1993 *Bigenerina nodosaria* d'Orbigny Sgarrella and Moncharmont Zei (p. 164, pl. 4, fig. 12)

***Brizalina alata* (Seguenza, 1862)**

1862 *Vulvulina alata* Seguenza (p. 115, pl. 2, fig. 5).

1991 *Brizalina alata* (Seguenza), Cimerman and Langer (p. 59, pl. 61, figs. 12–14)

***Brizalina catanensis* (Segunenza, 1862)**

1862 *Bolivina catanensis* Segunenza, (p.113, 125, pl.2, fig.3)

1993 *Bolivina catanensis* Segunenza, Sgarrella and Moncharmont Zei (p. 208, pl. 14, figs. 4-5)

2002 *Brizalina catanensis* (Segunenza), Kaminski et al (pl. 2, fig. 11)

***Brizalina spathulata* (Williamson, 1858)**

1858 *Textularia variabilis* var. *spathulata* Williamson (p. 76, pl. 6, figs. 164-165).

1991 *Brizalina spathulata* (Williamson), Cimerman and Langer (p. 60, pl. 62, figs. 3–5)

***Brizalina striatula* (Cushman 1922)**

1922 *Bolivina striatula* Cushman (p. 27, pl. 3, fig. 10)

1991 *Brizalina striatula* (Cushman) Cimerman and Langer (p. 60, pl. 62, figs. 6-9)

2002 *Brizalina striatula* (Cushman) Kaminski et al. (pl. 2, fig. 10)

***Bulimina aculeate* d'Orbigny, 1826**

1826 *Bulimina aculeata* d'Orbigny (p. 269)

1993 *Bulimina aculeata* d'Orbigny, Sgarrella & Moncharmont Zei (p. 211, pl. 15, fig. 1)

***Bulimina costata* d'Orbigny, 1852**

1852 *Bulimina costata* d'Orbigny (p. 194)

1993 *Bulimina costata* d'Orbigny Sgarrella and Moncharmont Zei (p. 211, pl. 15, fig. 3)

***Bulimina elongata* d'Orbigny, 1846**

1846 *Bulimina elongata* d'Orbigny (p. 187, pl. 11, figs. 19–20)

1993 *Bulimina elongata* d'Orbigny Sgarrella and Moncharmont Zei (p. 211, pl. 15, fig. 10-11)

2002 *Bulimina elongate* d'Orbigny, Kaminiski et al. (pl. 3, fig. 4)

***Bulimina marginata* d'Orbigny, 1826**

1826 *Bulimina marginata,* d'Orbigny (p. 269, pl. 12, figs. 10–12).

1991 *Bulimina marginata* d'Orbigny, Cimerman and Langer (1991, p. 62, pl. 64, figs. 9–11)

1993 *Bulimina marginata* d'Orbigny, Sgarrella and Moncharmont Zei (p. 212, pl. 15, figs. 5–7)

***Cassidulina carinata* Silvestri, 1896**

1896 *Cassidulina laevigata* d'Orbigny var. *carinata* Silvestri, (p. 104, pl. 2, figs. 10a-c)

1971 *Cassidulina carinata* Silvestri, Murray (p. 187, pl. 78, figs. 1-5)

1993 *Cassidulina carinata* Silvestri, Sgarrella and Moncharmont Zei (p. 236, pl. 23, figs. 8-9)

***Chilostomella mediterranensis* Cushman & Todd, 1949**

1949 *Chilostomella mediterranensis* Cushman & Todd (p. 92, pl. 15, fig. 25-26).

1993 *Chilostomella mediterranensis* Cushman & Todd, Sgarrella and Moncharmont Zei (p. 238, pl. 24, fig. 11)

***Discorbinella bertheloti* (d'Orbigny, 1839)**

1839 *Rosalina bertheloti* d'Orbigny (p. 135, pl. 1, figs. 28–30)

1993 *Discorbinella bertheloti* (d'Orbigny), Sgarrella and Moncharmont Zei (p. 216, pl. 16, figs. 11-12)

2002 *Discorbinella bertheloti* (d'Orbigny, 1839), Kaminiski et al. (pl. 5, figs. 1-2)

***Elphidium aculeatum* (d'Orbigny, 1846)**

1846 *Polystomella aculeate* d'Orbigny (p. 131, pl. 6, figs. 27–28)

1991 Elphidium aculeatum (d'Orbigny) Cimerman and Langer (p. 77, pl. 89, figs. 1–4)

***Elphidium complanatum* (d'Orbigny, 1839)**

1839 *Polystomella complanata* d'Orbigny (p. 129, pl. 2, figs. 35–36)

1993 *Elphidium complanatum* (d'Orbigny) Sgarrella and Moncharmont Zei (p. 228, pl. 20, figs .9–10)

***Elphidium crispum* (Linné, 1758)**

1758 *Nautilus crispus*, Linné (p. 709, pl. 1, fig. 2d-f)

1971 *Elphidium crispum* (Linné), Murray (p. 155, pl. 64, figs. 1-6)

1991 *Elphidium crispum* (Linné), Cimerman and Langer (p. 77, pl. 90, figs. 1–6)

***Elphidium macellum* (Fichtel & Moll, 1798)**

1798 *Nautilus macellus* var. *beta* Fichtel & Moll (p .66, pl. 10, figs. e-g, h–k)

1991 *Elphidium macellum* (Fichtel & Moll) Cimerman and Langer (p. 78, pl. 89, fig. 9)

2002 *Elphidium macellum* (Fichtel and Moll), Kaminski et al. (pl. 5, fig. 11)

***Favulina hexagona* (Williamson, 1848)**

1848 *Entosolenia squamosa* (Montagu) var. hexagona-Williamson (p. 20, pl. 2, fig. 23)

1991 *Favulina hexagona* (Montagu) Cimerman and Langer (p. 55, pl. 58, figs. 8-9)

***Fursenkonia acuta* (d'Orbigny, 1846)**

1846 *Polymorphina acuta* d'Orbigny (p. 234, pl. 13, figs. 4-5; pl. 14, figs. 5-7)

1993 *Fursenkoina acuta* (d'Orbigny) Sgarrella and Moncharmont Zei (p. 235, pl. 23, fig. 7)

2002 *Fursenkonia acuta* (d'Orbigny), Kaminski et al. (pl. 3, figs. 11-12)

***Globobulimina affinis* (d'Orbigny, 1839)**

1839 *Bulimina affinis* d'Orbigny (p. 105, pl. 2, figs. 25–26)

1993 *Globobulimina affinis* (d'Orbigny), Sgarrella and Moncharmont Zei (p. 212, pl.15, figs. 8–9)

2002 *Globobulimina affinis* (d'Orbigny), Kaminski et al. (pl. 3, fig. 8)

***Globocassidulina subglobosa* (Brady, 1884)**

1884 *Cassidulina subglobosa* Brady (p. 430, pl. 54, fig. 17 a–c)

1971 *Globocassidulina subglobosa* (Brady), Murray (p. 191, pl. 80, figs. 1-4)

1991 *Globocassidulina subglobosa* (Brady), Cimerman and Langer (p. 61, pl. 63, figs. 4–6)

***Haynesina depressula* (Walker & Jacob, 1798)**

1798 *Nautilus depressulus* Walker and Jacob (p. 641, fig. 33)

1971 *Nonion depressulum* (Walker and Jacob) Murray (p. 195, pl. 82, figs. 1-8)

2002 *Haynesina depressula* (Walker and Jacob) Kaminski et al. (pl. 4, figs. 4-5)

***Hyalinea balthica* (Schröter, 1783)**

1783 *Nautilus balthicus* Schroter (p. 20, pl. 1, fig. 2)

1993 *Hyalinea baltica* (Schroter) Sgarrella and Moncharmont Zei (p. 234, pl. 22, fig. 12)

2002 *Hyalinea baltica* (Schroeter) Kaminski et al. (pl. 3, fig. 13)

2004 *Hyalinea balthica* (Schroter) Meric et al. (pl. 27, fig. 3)

***Lagena striata* (d'Orbigny, 1839)**

1839 *Oolina striata* d'Orbigny (p. 21, pl. 5, fig. 12)

1991 *Lagena striata* (d'Orbigny) Cimerman & Langer (p. 53, pl. 55, figs. 6-7)

1993 *Lagena striata* (d'Orbigny) Sgarrella and Moncharmont Zei (p.198, pl.12, figs. 2-3)

***Lobatula lobatula* (Walker and Jacob, 1798)**

1798 *Nautilus lobatulus*, Walker and Jacob (p. 642, pl. 14, fig. 36)

1988 *Lobatula lobatula* (Walker and Jacob), Loeblich and Tappan (p. 168, pl. 637, figs. 10–13)

1991 *Lobatula lobatula* (Walker and Jacob), Cimerman and Langer (p. 71, pl. 75, figs. 1-4)

***Nonionella opima* Cushman, 1947**

1947 *Nonionella opima*, Cushman (p. 90, pl. 20, figs. 1-3)

1991 *Nonionella opima* Cushman, Cimerman and Langer (p. 74, pl. 84, figs. 1-3)

***Nonionella turgida* (Williamson, 1858)**

1858 *Rotalina turgida*, Williamson (p. 50, pl. 4, figs. 95–97)

1971 *Nonionella turgida* (Williamson), Murray (p. 193, pl. 81, figs. 1–5)

1991 *Nonionella turgida* (Williamson), Cimerman and Langer (p. 74, pl. 84, figs. 6–8)

***Planorbulina mediterranensis* d'Orbigny 1826**

1826 *Planorbulina mediterranensis* d'Orbigny (p. 280, no. 2)

1988 *Planorbulina mediterranensis* d'Orbigny, Loeblich and Tappan (p. 170, pl. 645, figs. 1–2)

1991 *Planorbulina mediterranensis* d'Orbigny, Cimerman and Langer (p. 71–72, pl. 78, figs. 1–8)

***Quinqueloculina seminulum* (Linné, 1758)**

1758 *Serpula seminulum* Linné (p. 786, pl. 2, fig. 1-a-c)

1971 *Quinqueloculina seminulum* (Linné) Murray (p. 64, pl. 24, figs. 1-6)

1991 *Quinqueloculina seminula* (Linné), Cimerman and Langer (p. 38, pl. 34, figs. 9–12)

***Rectuvigerina phlegeri* Le Calvez, 1959**

1959 *Rectuvigerina phlegeri* Le Calvez (p. 363, pl. 1, fig. 11)

1988 *Rectuvigerina phlegeri* Le Calvez, Alavi (pl. 1, fig. 4)

1993 *Rectuvigerina phlegeri* Le Calvez, Sgarrella and Moncharmont Zei (p. 215, pl. 16, figs. 3–4)

***Spiroloculina excavata* d'Orbigny, 1846**

1846 *Spiroloculina excavata* d'Orbigny, (p. 271, pl. 16, figs. 19–21)

1991 *Spiroloculina excavate* d'Orbigny, Cimerman and Langer (p. 30, pl. 23, figs. 1–3)

2002 *Spiroloculina excavata* d'Orbigny, Kaminski et al. (pl. 1, fig. 11)

***Textularia bocki* Höglund, 1947**

1947 Höglund (p. 171, pl. 12, figs. 5–6)

1991 *Textularia bocki* Höglund, Cimerman and Langer (p. 21, pl. 10, figs. 3–6)

2002 *Textularia bocki* Höglund, Kaminski et al. (pl. 1, figs. 1-2)

***Uvigerina mediterranea* Hofker, 1932**

1932 *Uvigerina mediterranea* Hofker (p. 118, p. 119, text figs. 32a-g)

1988 *Uvigerina mediterranea* Hofker Alavi (pl. 2, fig. 1)

1993 *Uvigerina mediterranea* Hofker, Sgarrella and Moncharmont Zei (p. 214, pl. 16, fig. 1-2)

***Valvulineria bradyana* (Fornasini, 1900)**

1900 *Discorbina bradyana* Fornasini (p. 393, fig. 43)

1991 *Valvulineria bradyana* (Fornasini) Cimerman and Langer (p. 64, pl. 67, figs. 8–10)

1993 *Valvulineria bradyana* (Fornasini), Sgarrella and Moncharmont Zei (p. 220, pl. 18, figs. 1–2)

720 **REFERENCES:**

721

722 Abbott, R.T., Dance, S.P. 1990. Compendium of seashells: a color guide to more than 4,200 of
723 the world's marine shells. 4th Edition. American Malacologists, Melbourne, Florida, USA,
724 411pp.

725 Aksu, A.E., Hiscott, R.N. and Yasar, D. 1999. Oscillating Quaternary water levels of the
726 Marmara Sea and vigorous outflow into the Aegean Sea from the Marmara Sea-Black Sea
727 drainage corridor. Marine Geology 153, 275-302.

728 Aksu, A.E., Hiscott, R.N., Kaminski, M.A., Mudie, P.J., Gillespie, H., Abrajano, T., Yasar, D.
729 2002. Last glacial-Holocene paleoceanography of the Black Sea and Marmara Sea: stable
730 isotopic, foraminiferal and coccolith evidence. Marine Geology 3160, 1-31.

731 Alavi, S.N. 1988. Late Holocene Deep-Sea Benthic Foraminifera from the Sea of Marmara.
732 Marine Micropaleontology 13, 213-237.

733 Algan, O., Çagatay, N., Tchepalyga, A., Ongan, D., Eastone, C., Gokasan, E. 2001. Stratigraphy
734 of the sediment infill in Bosphorus Strait: water exchange between the Black and
735 Mediterranean Seas during the last glacial Holocene. Geo-Marine Letters 20, 209-218.

736 Armijo R., Meyer B., Hubert A., Barka A. A. 1999. Westward propagation of the north
737 Anatolian fault into the northern Aegean: Timing and kinematics. Geology 27 267-270.

738 Armijo R., Meyer B., Navarro S., King G. C. P., Barka A. A. 2002. Asymmetric slip partitioning
739 in the Sea of Marmara pull-apart: a clue to propagation processes of the North Anatolian
740 Fault? Terra Nova 14, 80-86.

741 Armijo, R., Pondard, N., Meyer, B., Uçarkus, G., Mercier de Lepinay, B., Malavieille, J.,
742 Dominguez, S., Gustcher, M.-A., Schmidt, S., Beck, C., Çagatay, M. N., Çakir, Z., Imren,

743 C., Eris, K., Natalin, B., Özalaybey, S., Tolun, L. G., Lefèvre, I., Seeber, L., Gasperini, L.,
744 Rangin, C., Emre, Ö., Sarikavak, K. 2005. Submarine fault scarps in the Sea of Marmara
745 pull-apart (North Anatolian Fault): Implications for seismic hazard in Istanbul,
746 Geochemistry, Geophysics, Geosystems 6, Q06009.
747 Bahr, A., Lamy. F., Arz, H., Kuhlmann, H., Wefer, G. 2005. Late glacial to Holocene climate
748 and sedimentation history in the NW Black Sea. Marine Geology 214, 309-322.
749 Bard, E. Hamelin, B., Fairbanks, R.G., Zindler, A. 1990. Calibration of the 14C timescale over
750 the past 30,000 years using mass spectrometric U-Th ages from Barbados corals. Nature
751 345, 405-410.
752 Behl, R.J., Kennett, J.P. 1996. Brief interstadial events in the Santa Barbara Basin, NE Pacific,
753 during the past 60kar. Nature 379, 243-246.
754 Besiktepe, S.T., Sur, H.I., Ozsoy, E., Latif, M.A., Orguz, T., Unluata, A. 1994. The circulation
755 and hydrography of the Marmara Sea. Progress in Oceanography 34, 285-334.
756 Çagatay, M.N., Algan, O., Sakinç, M., Eastoe, C.J., Egesel, L., Balkis, N., Ongan, D., Caner, H.
757 1999. A mid-late Holocene sapropelic sediment unit from the southern Marmara sea shelf
758 and its paleoceanographic significance. Quaternary Science Reviews 18, 531-540.
759 Çagatay. M.N., Görür, N., Algan, A., Eastoe, C.J., Tchapalyga, A., Ongan, D., Kuhn, T., Kuscu,
760 I. 2000. Late Glacial-Holocene palaeoceanography of the Sea of Marmara timing of
761 connections with the Mediterranean and the black Sea. Marine Geology 167, 191-206.
762 Çagatay, M.N., Görür, N., Polonia, A., Demirbag, E., Sakinç, M., Cormier, M.-H., Capotondi,
763 L., McHugh, C.M.G., Emre, Ö., Eris, K. 2003. Sea-level changes and depositional
764 environments in the Izmit Gulf, eastern Marmara Sea, during the late glacial–Holocene
765 period. Marine Geology 202,159-173.

766 Caner, H., Algan, O. 2002. Palynology of sapropelic layers from the Marmara Sea. Marine
767 Geology 190, 35-46.
768 Cannariato, K.G., Kennett, J.P., Behl, R.J. 1999. Biotic response to late Quaternary rapid climate
769 switches in Santa Barbara Basin: Ecological and evolutionary implications. Geology 27,
770 63-66.
771 Cimmerman, F., Langer, M. R., 1991. Mediterranean Foraminifera. Slovenska Akdemija
772 Znanosti in Umetnosti. Classis IV: Historia Naturales dela Opera 30, Ljubljana. 119pp, 93
773 pls.
774 Cormier, M.-H., Seeber, L., McHugh, C.M.G., Polonia, A., Çagatay, M.N., Emre, O., Gasperini,
775 L., Görür, N., Bortoluzzi, G., Bonatti, E., Ryan, W.B.F., Newman, K. 2006. The North
776 Anatolian fault in the Gulf of Izmit (Turkey): Rapid vertical motion in response to minor
777 bends of a non-vertical continental transform. Journal of Geophysical Research 111,
778 doi:1029/2005JB003633, B04102.
779 Demirbag, E., Rangin, C., LePichon, X., Sengör, A.M.C. 2003. Investigation of the tectonics of
780 the Main Marmara Fault by means of deep-towed seismic data. Tectonophysics 361, 1-19.
781 Denton, G.H., Heusser, C.J., Lowell, T.V., Moreno, P.I., Anderson, B.G., Heusser, L.E.,
782 Schluchter, C., Marchant, D.R. 1999. Interhemispheric linkage of paleoclimate during the
783 last glaciation. Geografiska Annaler 81, 107-153.
784 Debenay, J. –P., Benetau, E., Zhang, J., Stouff, V., Geslin, E., Redois, F., Fernandez-Gonzalez, M.
785 1998. Ammonia beccarii and Ammonia tepida (Foraminifera); morphofunctional arguments
786 for their distinction. Marine Micropaleontology 34 (3, 235-244.
787 Dulk, M. den, Reichart, G.J., Heyst, S. van, Zwaan, G.J. van der, 2000. Benthic foraminifera as
788 proxies of organic matter flux and bottom water oxygenation? A case history from the
789 northern Arabian Sea. Palaeogeography, Palaeoclimatology, Palaeoecology 161, 337-359.

790 Ergin, M., Bodur, M.N., Ediger, V., 1991. Distribution of surficial shelf sediments in the
791 northeastern and southwestern parts of the Sea of Marmara: Strait and canyon regimes of
792 the Dardanelles and Bosporus. Marine Geology 96, 313-340.

793 Ergin, M. Nizamettin, K., Baki, V., Ozden, I., Levent, K., 1997. Sea-level changes and related
794 depositional environments on the southern Marmara Shelf. Marine Geology 140, 391.403.

795 Eris, K.K., Ryan, W.B.F., Çagatay, M.N., Sancar, U., Lercolais, G., Menot, G., Bard, E., 2007.
796 The timing and evolution of the post-glacial transgression across the Sea of Marmara shelf
797 south of Istanbul. Marine Geology 243, 57-76.

798 Evans, J.R., Austin, W.E.N., Brew, D.S., Wilkinson, I.P., Kennedy, H.A., 2002. Holocene shelf
799 sea evolution offshore northeast England. Marine Geology, 191, 147-164.

800 Fairbanks, R.G., 1989. A 17,000-year glacio-eustatic sea level record: influence of glacial
801 melting rates on the Younger Dryas event and deep-ocean circulation. Nature 342, 637-
802 642.

803 Fedorov, P.V. 1971. Postglacial transgression of the Black Sea. International Geology Review
804 14, 160-164.

805 Filipova-Marinova, M. Chirstova, R., Bozilova, E. 2004. Paleoecological conditions in the
806 Bulgarian Black Sea area during the Quaternary. Journal of Environmental
807 Micropaleontology, Microbiology and Meiobenthology 1, 135-154.

808 Fontanier C., Jorissen, F.J., Licari, L. et al., 2002. Live benthic foraminiferal faunas from the
809 Bay of Biscay: faunal density, composition, and microhabitats. Deep-Sea Research I 49,
810 751-785.

811 Fontanier, C., Jorissen, F.J., Chaillou, G. et al., 2003. Seasonal and interannual variability of
812 benthic foraminiferal faunas at 550m depth in the Bay of Biscay. Deep-Sea Research I, 50,
813 457-494.

814 Giosan, L. Mart, Y., McHugh, C.M., Vachtman, D., Çagatay, N.M., Kadir, E.K., Ryan, W.B.
815 2005. Megafloods in Marginal Basins: New Data from the Black Sea. EOS Trans. AGU 86
816 (52): PP32A-03.
817 Gokasan, E., E. Demirbag, F.Y. Oktay, B. Ecevitoglu, M. Simsek, and H. Yüce. 1997. On the
818 origin of the Bosphorus. Marine Geology 140, 183-199.
819 Gökasan E., Algan, O., Tur, H., Meriç, E., Türker, A., Simsek, M. 2005. Delta formation at the
820 southern entrance of Istanbul Strait (Marmara sea, Turkey): a new interpretation based on
821 high-resolution seismic stratigraphy. Geo-Marine Letters 25, 370-377.
822 Gökasan E., Ergin, M. Ozyalvac, M., Ibrahim Sur, H., Tur, H., Görum, T., Ustaömer, T. Gul
823 Batuk, F., Alp. H., Birkan, H., Turker, A., Gezgin, E., Ozturan, M. 2008. Factors
824 controlling the morphological evolution of the Canakkale Strait (Dardanelles, Turkey).
825 Geo-Mar Letters 28, 107-129.
826 Görür, N., M.N. Çagatay, M. Sakinç, M. Sümengen, K. Sentürk, C. Yaltirak, and A. Tchapalyga.
827 1997. Origin of the Sea of Marmara as deduced from Neogene to Quaternary
828 Paleogeographic evolution of its frame. International Geology Review 39, 342-352.
829 Grosswald, M.G. 1980. Late Weichselian ice sheet of Northern Europe. Quaternary Research 13,
830 1-32.
831 Grosswald, M.G. 1998. Late-Weichselian ice sheets in Arctic and Pacific Siberia. Quaternary
832 International 45-46, 3-18.
833 Gurung, D., McHugh, C.M., Ryan, W.B., Giosan, L., Mart, Y., Çagatai, N. 2006. Late
834 Pleistocene-Holocene climate change inferred from fossil fauna in the Marmara Sea,
835 Turkey. 2006. EOS Trans. AGU 87 (52), PP23B-1748.
836 Haynes, J. R. 1981. Foraminifera. John Wiley & Sons, New York 433pp.

837 Hayward, B., Buzas, M.A., Buzas-Stephens, P., Holzman, M., 2003. The lost types of *Rotalia*
838 *Beccarii* var *tepida* Cushman 1926. J. Foraminifer. Res. 33, 352-354.
839 Hiscott, R.N., Aksu, A.E., Yasar, D., Kaminski, M.A., Mudie, P.J., Kostylev, V.E., MacDonald,
840 J.C., Iser, F.I., Lord, A.R. 2002. Deltas south of the Bosphorus Strait record persistent
841 Black Sea outflow to the Marmara Sea since ~10ka. Marine Geology 190, 95-118.
842 Hiscott, R.N., Aksu, A.E., Mudie, P.J., Kaminski, M., Abrajano, T., Yasar, D., Rochon, A. 2006.
843 The Marmara Sea Gateway since ~16Ka: non-catastrophic causes of paleoceanographic
844 events in the Black Sea at 8.4 and 7.15 ka. In: Yanko-Hombach, V. Gilbert, A.S., Panin,
845 N., Dolukhanov, P. (Eds.), The Black Sea Floor Question: Changes in Coastline, Climate
846 and Human Settlement. Springer, Dordrecht, The Netherlands.
847 Hughen, K. A., Overpeck, L.C., Anderson, R.F. 1996. The nature of varved sedimentation in the
848 Cariaco Basin, Venezuela, and its palaeoclimatic significance, in Palaeoclimatology and
849 Palaeoceanography from Laminated Sediments, edited by A. E. S. Kemp, pp. 171-183,
850 Geological Society, London.
851 Itou, M., Matsumura, I., Noriki, S. 2000. A large flux of particulate matter in the deep Japan
852 Trench observed just after the 1994 Sanriku-Oki earthquake, Deep-Sea Research I 4,
853 1987-1998.
854 Kaiho, K. 1994. Benthic foraminiferal dissolved-oxygen index and dissolved-oxygen levels in
855 the modern ocean. Geology 22, 719-722.
856 Kaminski, M.A., Aksu, A., Box, M., Hiscott, R.N., Filipescu, S., Al-Salameen, M. 2002. Late
857 Glacial to Holocene benthic foraminifer in the Marmara Sea: implications for Black Sea-
858 Mediterranean Sea connections following the last deglaciation. Marine Geology 19, 165-
859 202.
860 Lane-Serff, G.E., Rohling, E.J., Bryden, H., Charnock, H. 1997. Postglacial connection of the
861 Black Sea to the Mediterranean and its relation to the timing of sapropel formation.

Palaeoceanography 12, 169-174.

Lee, J. J., Pawlowski, J., Debenay, J. P., Whittaker, J. E., Banner, F. T., Gooday, A. J., Tendal, O., Haynes, J., Faber, W. W. 2000. Class Foraminifera In: J. J. Lee, G. F. Leedale, P. Bradbury (eds.). An Illustrated Guide to the Protozoa, 2nd Edition. Society of Protozoologists. Allen Press, Lawrence Kansas, 877-951.

Le Pichon X., Sengör A. M. C., Demirbag E., Rangin C., Imren C., Armijo R., Görür N., Çagatay M. N., Mercier de Lepinay B., Meyer B., Saatçilar R., Tok B. 2001. The active main Marmara fault. Earth and Planetary Science Letters 192, 595-616.

Leventer, A., Williams, D.F., Kennett, J.P. 1982. Dynamics of the Laurentide ice sheet during the last deglaciation: evidence from the Gulf of Mexico. Earth and Planetary Science Letters 59, 11-17.

Loeblich, A. R., Tappan, H. 1988. Foraminiferal Genera and their Classification, vol. 1-2. Van Nostrand Reinhold, New York 970 pp., 847 pl.

Major, C.O., Ryan, W., Lercolais, G., Hajdas, I. 2002. Constraints on Black Sea outflow to the Sea of Marmara during the last glacial-interglacial transition. Marine Geology 190, 19-34.

Major, C.O., Goldstein, S.L., Ryan, W.B.F., Lercolais, G., Piotrowski, A.M., Hajdas, I. 2006. Quaternary Science Reviews 25, 2031-2047.

Mangerud, J., Andersen, S.T., Berglund, B.E., Donner, J.J. 1974. Quaternary stratigraphy of Norden, a proposal for terminology and classification. Boreas 3, 109-127.

Malcolm, S.J., Price, N.B., 1984. The behaviour of iodine and bromine in estuarine surface sediments. Mar. Chem. 15, 263–271.

883 Mart, Y., Ryan, W., Çagatay, N., McHugh, C., Giosan, L., Vachtman, D., 2006, Evidence for
884 intensive flow from the Bosporus northwards during the early Holocene. EGU Geophysical
885 Research Abstracts, V. 8, 02572.
886 McHugh, C. M. G., Seeber, L. , Cormier, M.-H., Dutton, J., Çagatay, M. N., Polonia, A., Ryan,
887 W. B. F., Görür, N. 2006. Submarine earthquake geology along the North Anatolian Fault
888 in the Marmara Sea, Turkey: A model for transform basin sedimentation. Earth and
889 Planetary Science Letters 248, 661-684. doi:10.1016/j.epsl.2006.05.038
890 Meric, E., Avsar, N., Bergin, F. 2004. Benthic foraminifera of Eastern Aegean Sea (Turkey)
891 systematics and autoecology. Chamber of Geological Engineers of Turkey and Turkish
892 Marine Research Foundation, 18, 306pp.
893 Meric, E., Algan, O. 2007. Paleoenvironments of the Marmara Sea (Turkey) Coasts from
894 paleontological and sedimentological data. Quaternary International 167, 128-148.
895 Mudie, P.J., Aksu, A.E., Yasar, D. 2001. Late Quaternary dinoflagellate cysts from the Black,
896 Marmara and Aegean seas: variations in assemblages, morphology and paleosalinity.
897 Marine Micropaleontology 43, 155-178.
898 Mudie, P.J., Rochon, A., Aksu, A.E., 2002. Pollen stratigraphy of Late Quaternary cores from
899 Marmara Sea: land-sea correlation and paleoclimatic history. Marine Geology 190, 233-
900 260.
901 Mudie, P.J., Marret, F., Aksu, A.E., Hiscott, R.N., Gillespie, H. 2007. Palynological evidence for
902 climatic change, anthropogenic activity and outflow of Black Sea water during the late
903 Pleistocene and Holocene: Centennial- to decadal-scale records from the Black and
904 Marmara Seas. Quaternary International 167, 73-90.
905 Murray, J. W. 1971. An atlas of British recent foraminiferids. American Elsevier Publications,
906 New York. 244pp.

907 Murray, J. W., 1986. Living and dead Holocene foraminifera of Lyme Bay, Southern England.
908 Journal of Foraminiferal Research 16:347-352.
909 Murray, J. 1991. Ecology and Palaeoecology of Benthic Foraminifer. Longman Scientific &
910 Technical. 397pp.
911 Murray, J. 2006. Ecology and Applications of Benthic Foraminifera. Cambridge University
912 Press. 422pp.
913 Myers, P.G., Wielki, C., Goldstein, S.B., Rohling, E.J., 2003. Hydraulic calculations of
914 postglacial connections between the Mediterranean and the Black Sea. Marine Geology
915 201, 253-267.
916 Newman, K. R. 2003. Using submerged shorelines to constrain recent tectonics in the Marmara
917 Sea, northwestern Turkey. Department of Geology, Senior Thesis, Smith College: 49pp.
918 Okay, A.I., Demirbag, E., Kurt, H., Okay, N., Kusçu, I. 1999. An active, deep marine strike-slip
919 basin along the North Anatolian fault in Turkey. Tectonics 18, 129-147.
920 Okay, N., Ergun, B. 2005. Source of basinal sediments in the Marmara Sea investigated using
921 heavy minerals in the modern beach sands. Marine Geology 216, 1-15.
922 Ortiz, J.D., O'Connell, S.B., DelViscio, J., Dean, W., Carriquiry, J.D., Marchitto, T., Zheng, Y.,
923 vanGeen, A. 2004. Enhanced marine productivity off western North America during warm
924 climate intervals of the past 52 k.y. Geology 32, 521-524.
925 Peterson, L. C., Overpeck, J.R., Kipp, N.G., Imbrie, J. 1991. A high-resolution late Quaternary
926 upwelling record from the anoxic Cariaco Basin, Venezuela. Paleoceanography 6, 99-119.
927 Phleger, F. 1960. Ecology and distribution of Recent foraminifera. John Hopkins Press.
928 Baltimore, MD, 297 pp.
929 Polonia A., Cormier M.H., Çagatay M.N., Bortoluzzi G., Bonatti E., Gasperini L., Seeber L.,

930 Görür N., Capotondi L., McHugh C.M.G., Ryan W.B.F., Emre O., Okay N., Ligi M., Tok
931 B., Blasi A., Busetti M., Eris K., Fabretti P., Fielding E.J., Imren C., Kurt H., Magagnoli
932 A., Marozzi G., Ozer N., Penitenti D., Serpi G., Sarikavak K., 2002, Exploring submarine
933 earthquake geology in the Marmara Sea, EOS Transactions AGU 83 229, 235-236.
934 Polonia, A., Gasperini, L., Amorosi, A., Bonatti, E., Bortoluzzi, G., Çagatay, M. N., Capotondi,
935 L., Cormier, M.-H., Görür, N., McHugh, C. M. G., Seeber, L. 2004 Holocene slip rate of
936 the North Anatolian Fault beneath the Sea of Marmara. Earth and Planetary Science Letters
937 227, 411-426.
938 Rangin, C., Demirbag, E., Imren, C., Crusson, A., Normand, A., Le Drezen, E., Le Bot, A. 2001.
939 Marine Atlas of the Sea of Marmara: Ifremer.
940 Reichel, T. and Halbach, P. 2007. An authigenic calcite layer in the sediments of the Sea of
941 Marmara-A geochemical marker horizon with paleoceanographic significance. Deep Sea
942 Research II 54, 1201-1215.
943 Renberg, I., 1990. A procedure for preparing large sets of diatom slides form sediment cores.
944 Journal of Paleolimnology 4, 87-90.
945 Ross, D. A., Degens, E. T. 1974. Recent sediments of the Black Sea, (Eds.) E. T. Degens, D. A.
946 Ross, The Black Sea Geology, Chemistry and Biology, Tulsa: Am. Assoc. Petrol. Geol.
947 Mem. 20, 183-199.
948 Rossignol-Strick, M. 1995. Sea-land correlation of pollen records in the eastern Mediterranean
949 for the glacial-interglacial transition: Biostratigraphy versus radiometric time-scale.
950 Quaternary Science Reviews 14, 893-915.
951 Round, F.E.E., Crawford, R.M., Mann, D.G. 1990. Diatoms: Biology and Morphology of the
952 Genera. Cambridge University Press 560pp.

953 Ryan, W.B.F., Pitman, W.C., Major, C.O., Shimkus, K., Moskalenko, V., Jones, G.A., Dimitrov,
954 P., Görür, N., Sakinç, M., Yüce, H. 1997. An abrupt drowning of the Black Sea shelf.
955 Marine Geology 138, 119-126.
956 Ryan, W.B.F., Major, C.O., Lericolais, G., and Goldstein, S. L. 2003. Catastrophic flooding of
957 the Black Sea. Annual Review Earth Planetary Science 31, 525–254.
958 Schonfeld, J. 1997. The impact of the Mediterranean Outflow Water (MOW) on benthic
959 foraminiferal assemblages and surface sediments at the southern Portuguese continental
960 margin. Marine Micropaleontology 29, 211-236.
961 Schonfeld, J. 2001. Benthic foraminifera and pore-water oxygen profiles: a re-assessment of
962 species boundary conditions at the western Iberian margin. Journal of Foraminiferal
963 Research 31, 86-107.
964 Sengör, A.M.C., Görür, N., Saroglu, F. 1985. Strike-slip faulting and related basin formation in
965 zones of tectonic escape: Turkey as a case study, in Strike-Slip Deformation, Basin
966 Formation, and Sedimentation, edited by K.T. Biddle, and N. Christie-Blick. Soc. Econ.
967 Paleont. Min. pp. 227-264
968 Sen Gupta, B.K., Machain-Castillo, M.L. 1993. Benthic foraminifera in oxygen-poor habitats.
969 Marine Micropaleontology 20, 183-201.
970 Sen Gupta, B.K., Turner, R.E., Rabalis, N.N. 1996. Seasonal oxygen depletion in continental-
971 shelf waters of Louisiana- Historical record of benthic foraminifers. Geology 24, 227-230.
972 Sgarella, F., Moncharmont Zei, M. 1993. Benthic foraminifera of the Gulf of Naples (Italy):
973 Systematics and autoecology. Boll. Soc. Paleontologist Italy 32, 145-264.
974 Sidall, M., Rohling, E.J., Almogi-Labin, A., Hemleben, Ch., Meischner, D., Schmelzer, I.,
975 Smeed, D.A. 2003. Sea-level fluctuations during the last glacial cycle. Nature 423, 853-
976 858.
977 Sidall, M., Lawrence, J. P., Helfrich, K. R., Giosan, L. 2004. Testing the physical oceanographic

implications of the suggested sudden Black Sea infill 8400 years ago. Paleoceanography 19, PA1024, doi:10.1029/2003PA000903.

Siani, G., Paterne, M., Arnold, M., Bard, E., Metivier, B., Tisnerat, N., Bassinot, F. 2000. Radiocarbon reservoir ages in the Mediterranean Sea and Black Sea, Radiocarbon 42, 271-280.

Sperling, M., Schmiedl, G., Hembleben, Ch., Emeis, K.C., Erlenkeuser, H., Grootes, P.M. 2003. Black Sea impact on the formation of eastern Mediterranean sapropel S1? Evidence from the Marmara Sea. Palaeogeography, Palaeoclimatology, Palaeoecology 190, 9-21.

Stanley, D.J., Blanpied, C. 1980. Late Quaternary water exchange between the eastern Mediterranean and the Black Sea. Nature 266, 537-541.

Stuvier M., and Reimer, P.J., 1993. Extended 14C database and revised CALIB radiocarbon calibration program. Radiocarbon 35, 215-230.

Svitoch, A.A., 1999. Caspian Sea level in the Pleistocene: hierarchy and position in the paleogeographic and chronological records. Oceanology 39, 94-101.

Thomas E., Gapotchenko T., Varekamp J., Mecray E.L., Buchholtz ten Brink M.R. 2000. Benthic foraminifera and environmental changes in Long Island Sound. Journal of Coastal Research 16, 641-655.

Thunell, R.C., Williams, D.F. 1989. Glacial-Holocene salinity changes in the Mediterranean Sea: hydrographic and depositional effects. Nature 338, 493-496.

Thunell, R., Tappa, E., Varela R., Llano, M., Astor, Y., Muller-Karger, F., Bohrer, R. 1999. Increased marine sediment suspension and fluxes following an earthquake. Nature 398, 233-236.

Tyson, R.V., Pearson, T.H. 1991. Modern and ancient continental shelf anoxia: an overview. Geological Society Special Publication 58, 1-24.

1002 Vaught, K.C., Abbott, R.T., Boss, K.J. 1989. Classification of the living Mollusca. American
1003 Malacologist. Melbourne, Fla. U.S.A., 204pp.
1004 Yanko, V. V., Troitskaja, T. S. 1987. Pozdne-chetvertichnye foraminifery Chernogo morya. Late
1005 Quaternary Foraminifera of the Black Sea. Akademiya Nauk SSSR. Institut Geologii I
1006 Geofiziki Trudy 694, 111pp.
1007
1008
1009

1009 FIGURE CAPTIONS:

1010

1011 Figure 1. (a). Satellite image of the Aegean Sea, Marmara Sea and Black Sea corridor showing
1012 Marmara's significant location as a gateway between the Aegean and Black Seas, and the
1013 location of the Dardanelles and Bosporus Straits. (b) Multibeam bathymetry of the main
1014 Marmara Sea basins (Rangier et al., 2001). Boxes show the location of the studied areas in
1015 Imrali, Prince Islands and **Ç**ekmece.

1016

1017 Figure 2. Multibeam bathymetry of the Imrali study area showing the location of high resolution
1018 subbottom profiles, CHIRP, navigation tracks (red lines) and location of core transect (red dots).
1019 The studied cores IM05 and IM03 are located at -152 and -298 m of water depth, respectively.
1020 The Marmara Lake high-stand was at -85 m (Çagatay et al., 2000; Algan et al., 2001; Newman,
1021 2003).

1022

1023 Figure 3. (a). Multibeam bathymetry of the Imrali study area showing the location of the cores
1024 and CHIRP subbottom profile (Line imc04-06). Modified after McHugh et al., 2006. (b). CHIRP
1025 subbottom profile extending from -90 to -200 m. Offsets due to normal fault activity are 15 m
1026 and 1.5 m. Also shown an offset of 13.5 m due to possibly slumping and/or related fault activity.
1027 (c). After reconstruction of fault related offsets, Core IM05 is located at -115 m, there is a
1028 paleoshoreline at -95 m, and the lake high-stand paleoshoreline at -87 m. Correlation of the
1029 lithology and age to the seismic line reveals the lacustrine-marine transition occurred at ~12.0 ka
1030 BP (brown reflector). Turquoise surface delineates the sea-floor and sediment deposited during
1031 the Holocene.

Figure 4. Lithology and facies of Core IM05 showing the lacustrine barren stage (Facies 1, 400-365 cm) and lacustrine fertile (Facies 2, 365-275 cm). The transition from lacustrine to marine (Facies 3) is marked by a bed of coarse sand with flat, well-rounded pebbles, and sand laminae above (275 to 260 cm). Marine muds and fauna characterize the core from 260 to 0 cm (Facies 4).

Figure 5. Sedimentation rates calculated from the slope of the line for Core IM05 and Core 6 on the Imrali and Prince Islands margin, respectively. Sedimentation rates for the lacustrine stage are two orders of magnitude greater than the marine. Sedimentation rates for the Holocene are comparable for the southern and northern margins.

Figure 6. The physical properties of Core IM05 (p-wave velocity, bulk density, and magnetic susceptibility) show the changes that occurred from the barren lake stage (Facies 1), to the fertile lake (Facies 2), due to the marine incursion (Facies 3) to fully marine conditions (Facies 4).

Figure 7. Benthic and planktonic foraminferal assemblages from the Imrali outer shelf exhibit major faunal and ecological shifts due to rapidly changing environmental conditions. Most foraminifers are grouped by genus due to the similar ecological preferences of species (*Bulimina spp., Brizalina spp.*) *A. tepida* is restricted to shallow water, marsh environments while *A. beccarii* is a highly adaptable species. *H. balthica* is associated to stratification of the water column. *G. affinis* equates with high organic flux and productivity. Ages are reported as

radiocarbon, calibrated, and some (at 150 and 25 cm) were calculated from the sedimentation rates of 0.02 cm/yr.

Figure 8. (a). Stable oxygen isotope records of Cores IM05 and IM03. Ages are shown as calibrated years BP. Both cores isotope values range from 2.2 to 1.2 δ18O‰ and show an overall trend to lighter values interpreted as warming and freshening. Heavy values in both cores are interpreted as a high salinity and low temperature signal. (b). Correlation of carbon isotopes between Cores IM05 and IM03. Both cores show an overall trend to less depleted values from -2.5 to -0.5 $\delta^{13}C$ and uniform values after ~6ka BP.

Figure 9. (a). Sediment coring sites along the outer shelf of Prince Islands. Water depth contours are given in meters. (b). Subbottom profile (CHIRP) showing a -92 m terrace, lacustrine surface (brown), and marine Holocene sediments above (blue). The age of the sediments above the lacustrine surface, ~12 ka BP, is in calibrated years.

Figure 10. Lithostratigraphic columns for Cores 8, 6, 5, and 7 recovered from the Prince Islands outer shelf. The sediments are generally sandy towards the base of the cores where they contain reworked lacustrine and marine shells indicating that the lacustrine- marine transition was very close but not penetrated by the cores possibly due to indurated or sandier strata. The sediments fine upwards to silty clays and contain marine faunas. Ages reported in calibrated years BP.

Figure 11. Foraminiferal species in Core 6. The low oxygen concentration foraminifers are represented by *Bulimina spp., Brizalina spp.* and by *C. carinata*. *Bulimina aculeata* dominates

Bulimina spp. and *Brizalina spathulata* and *Brizalina catanensis* dominate the *Brizalina spp*. As in Core IM05, *C. carinata* is the first colonizer after the marine incursion. The marsh shallow water foraminifers are represented by *Elphidium spp. (E. crispum, E. articulatum, E. macellum)* and *Ammonia spp*. (*A. tepida, A. compacta, A. beccarii*). After the initial marine incursion *A. tepida*, the marsh shallow water species, disappears and *Elphidium spp*. greatly diminishes in abundance. A homogenite deposit is present from 150 to 100 cm, Post 6 ka BP the environment becomes stable as shown by the lack of changes in foraminifers.

Figure 12. Br content estimated from XRF scanning data (in counts/sec). (a). Cores scanned from the Prince Islands shelf. (b). Cores scanned from the northern shelf (Çekmece). Values indicate freshwater-derived organic matter (less than 200 counts/sec), whereas higher than that limit are indicative of marine organic matter. Calibrated dates at their corresponding levels in the cores are also shown.

Figure 13. Calcium carbonate wt% for the Prince Islands and Çekmece cores. Values are greatest (25-40wt%) during the lacustrine stage and immediately above the marine incursion.

Figure 14. (a). Water depth in meters and core location along the Çekmece outer shelf. (b). Subbottom profile (CHIRP) showing the -87 m high-stand lake plaeoshoreline, a -92 m paleoshoreline, the late Pleistocene lacustrine surface (brown), and marine Holocene sediments above (turquoise surface).

1099 Figure 15. Lithostratigraphic columns of cores taken in the northern Çekmece margin between -
1100 93 and -118 m of water depth. Mollusk assemblages (*Dreissena sp.*, *Theodoxus sp.*) indicate
1101 lacustrine sediments in Core 2 from 50 to 123 cm and at the base of Core 1. Ages are reported in
1102 calibrated years BP. Lacustrine sediments are silt rich and contain charcoal fragments.
1103 Unfossiliferous layers of indurated clays, possibly diagenetically altered by carbonate
1104 cementation, separate the lacustrine and marine sediments. Marine sediments are primarily
1105 composed of silty clays with abundant marine mollusks and benthic and planktonic foraminifers.
1106 Cores 1 and 3 are sandier and contain reworked intervals manifested by the old over young ages
1107 and the mixing of marine and lacustrine shells.
1108
1109 Figure 16. Benthic and planktonic foraminiferal assemblages from the Çekmece outer shelf
1110 exhibit similar ecological shifts as those of Imrali and Prince Island shelves. Core 1 as in Core 6
1111 shows the low oxygen concentration foraminifers dominated by *B. aculeata*, *B. spathulata*, *B.*
1112 *catanensis*, and *C. carinata*. A marsh shallow water environment is indicated by *A. tepida* and *E.*
1113 *crispum* that dominates the *Elphidium spp*. *Hyalinea balthica* and *Globobulimina affinis* show
1114 shifts in their abundance from approximately 11.5 to 8.2 ka BP possibly related to the Younger
1115 Dryas and Black Sea outflow.
1116
1117 Figure 17. Summary of the lithostratigraphy and biostratigraphy correlated to a calibrated
1118 radiocarbon chronology permits to reconstruct a sequence of events for the Black Sea-Marmara-
1119 Mediterranean corridor as documented by this study. The bases of the lithostratigraphic
1120 sequences provide evidence for Marmara Lake during glacial times. From ~ 15.5 ka BP to 14.5
1121 ka BP the lake was supplied with glacial meltwaters from the Black Sea (a lake at this time) that

1122 spilled into the Marmara Lake and into the Aegean Sea. The Bolling-Allerod brought warm
1123 conditions to Marmara Lake from ~14.5 ka to 13.0 ka. Evaporative conditions prior to the marine
1124 incursion could have contributed to a lake drawdown with formation of the -95 m terrace, which
1125 could have also been formed by wave erosion. The incursion of marine waters into Marmara Sea
1126 occurred at 12 ka BP. At this time the Black Sea was either isolated or provided a very weak
1127 outflow to Marmara Sea. A standstill was documented from ~11.5 to 10.5 ka BP and interpreted
1128 as the Younger Dryas event. Sea-level continued to rise and there is evidence for strong outflow
1129 from the Black Sea at ~9.2 ka BP. The modern two-layer circulation was well established by 6
1130 ka BP when sea level reached close to the present shoreline.

Table 1. Radiocarbon and calibrated ages for the studied cores.

Core I.D.	Depth mbsf	Core Int. (cm)	Type	Mollusk	14C Age	Age Error	*Calibrated age ka
MedEx05-1	102.60	60	mollusk	*Corbula sp.*	10600	45	11.73
MedEx05-1	102.95	95	foraminifera		9910	60	10.74
MedEx05-1	103.00	100	mollusk	*Corbula sp.*	10500	50	11.52
MedEx05-2	93.95	30	mollusk	*Lucinella sp.* *Gouldia sp.*	8760	55	9.36
MexEx05-3	93.20	20	mollusk	*Lucinella sp.* *Gouldia sp.*	5000	40	5.26
MexEx05-3	93.25	25	mollusk	*Lucinella sp.* *Gouldia sp.*	10300	50	11.21
MedEx05-3	93.50	50	foraminifera		6900	35	7.35
MexEx05-5	93.00	70	mollusk	*Lucinella sp.* *Gouldia sp.*	9890	50	10.70
MexEx05-5	93.10	80	mollusk	*Lucinella sp.* *Gouldia sp.*	10450	80	11.46
MedEx05-6	98.5	100	foraminifera		5350	45	5.64
MedEx05-6	99.10	160	foraminifera		9280	60	10.00
MedEx05-6	99.25	175	mollusk	*Lucinella sp.* *Gouldia sp.*	9720	55	10.50
MedEx05-6	99.52	202	mollusk	*Corbula sp.*	10600	40	11.74
Core IM03	299.60	150	foraminifera		5260	50	5.50
	300.40	230	foraminifera		5420	80	5.72
Core IM05	152.15	55	foraminifera		3440	25	3.24
	152.60	100	foraminifera		4700	40	4.85
	152.60	200	foraminifera		8590	40	9.15
	154.05	245	mollusk	clam	11500	75	12.95**
	154.15	254	foraminifera		10350	45	11.25
	154.21	260	mollusk	clam	10650	40	11.83
	154.55	295	mollusk	*Dreissena sp.*	13000	65	14.66
	155.14	354	mollusk	*Dreissena sp.*	13150	60	14.95

*Calibrated ages were obtained by applying Sinai et al. (2000) reservoir corrections and converted to calendar years with the CALIB 5.0 program (Stuvier and Reimer, 1993).
**Possibly reworked.

Figure 1

(a)


Black Sea
Bosporus Strait
Marmara Sea
Ægean Sea
Dardanelles Strait

(b)

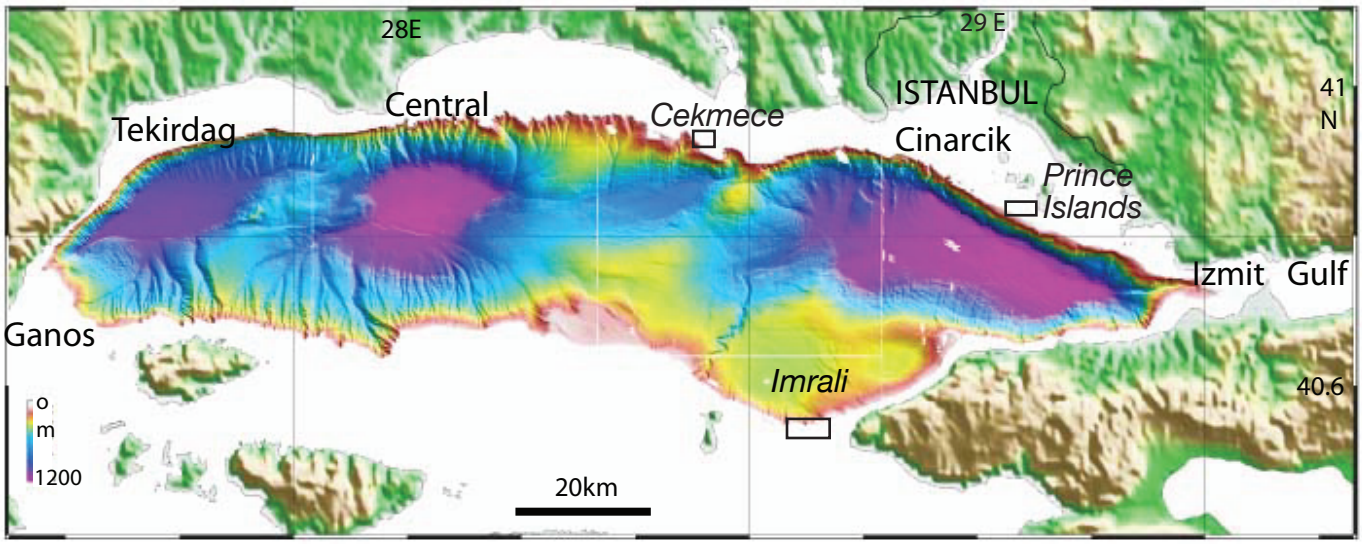
28E
29 E
Central
Tekirdag
Cekmece
ISTANBUL
Cinarcik
41
N
Prince
Islands
Izmit
Gulf
Ganos
Imrali
40.6
o
m
1200
20km

Figure 2.

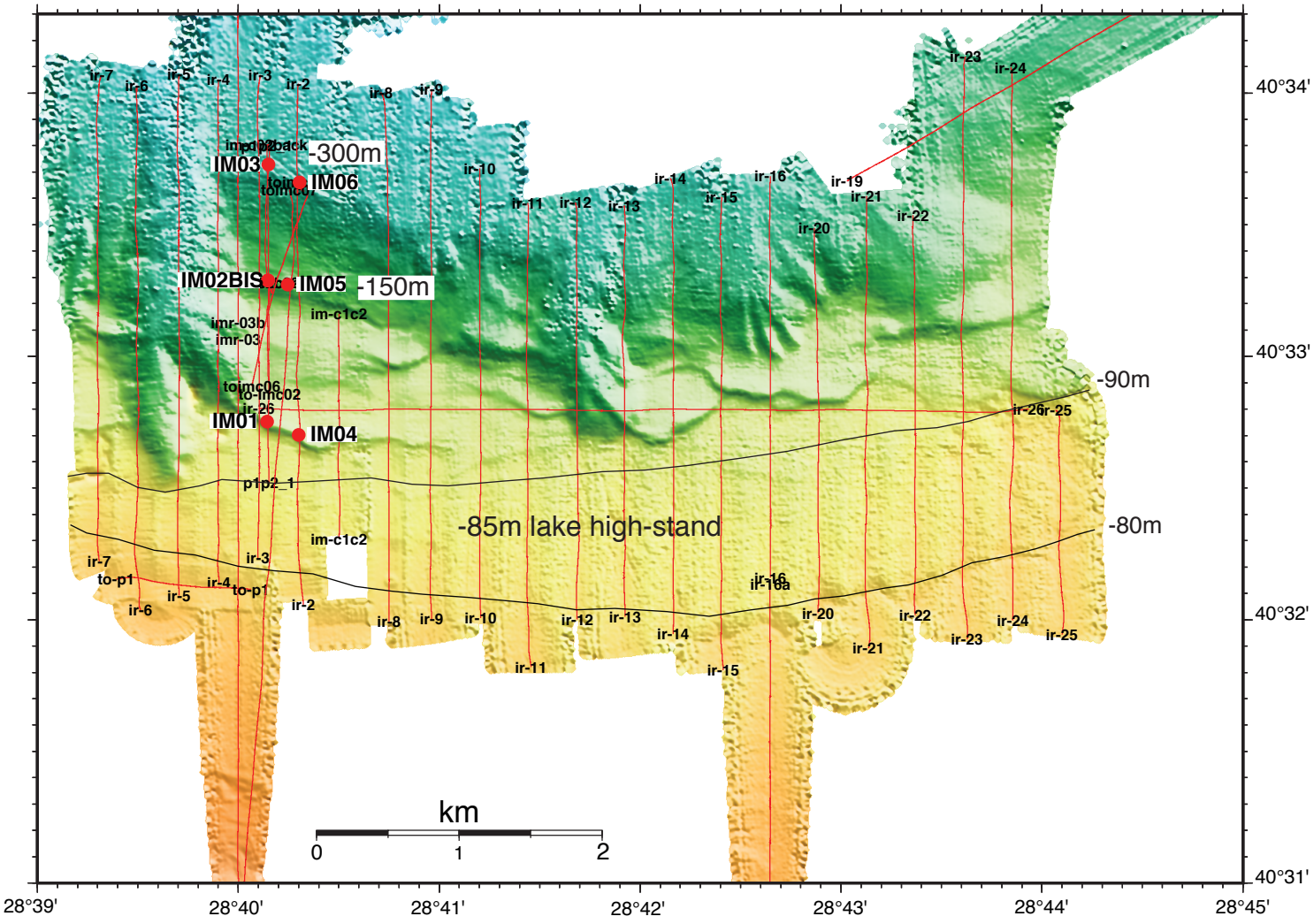
IM03
IM06
IM02BIS
IM05
IM01
IM04
-300m
-150m
-90m
-80m
-85m lake high-stand
im-c1c2
imr-03b
imr-03
p1p2_1
km
0
1
2
40°34'
40°33'
40°32'
40°31'
28°39'
28°40'
28°41'
28°42'
28°43'
28°44'
28°45'

Figure 3

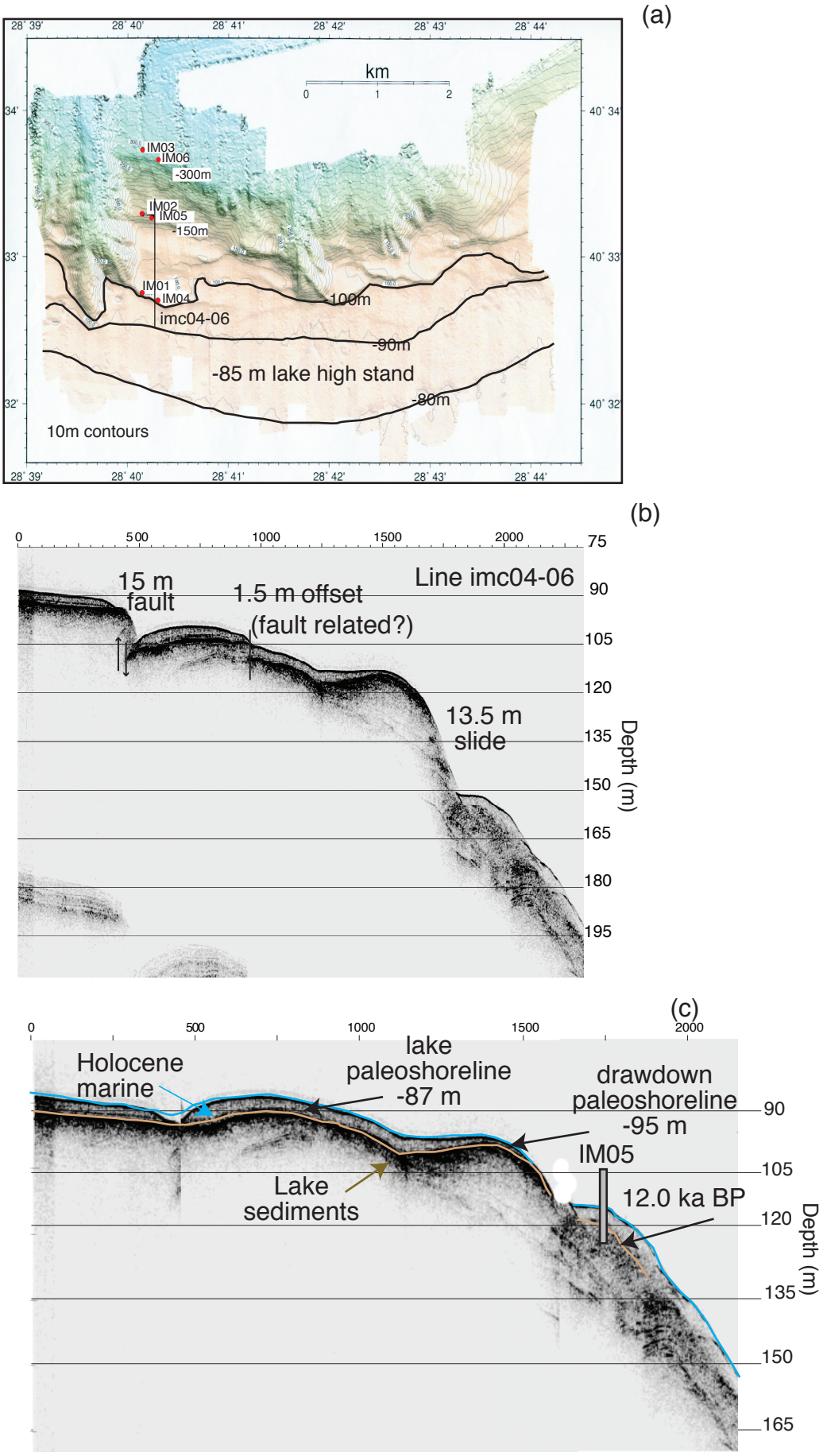
(a)
km
0
1
2
IM03
IM06
-300m
IM02
IM05
-150m
IM01
IM04
imc04-06
-100m
-90m
-85 m lake high stand
-80m
10m contours
(b)
Line imc04-06
15 m fault
1.5 m offset (fault related?)
13.5 m slide
Depth (m)
(c)
Holocene marine
lake paleoshoreline -87 m
drawdown paleoshoreline -95 m
IM05
12.0 ka BP
Lake sediments
Depth (m)

Figure 4

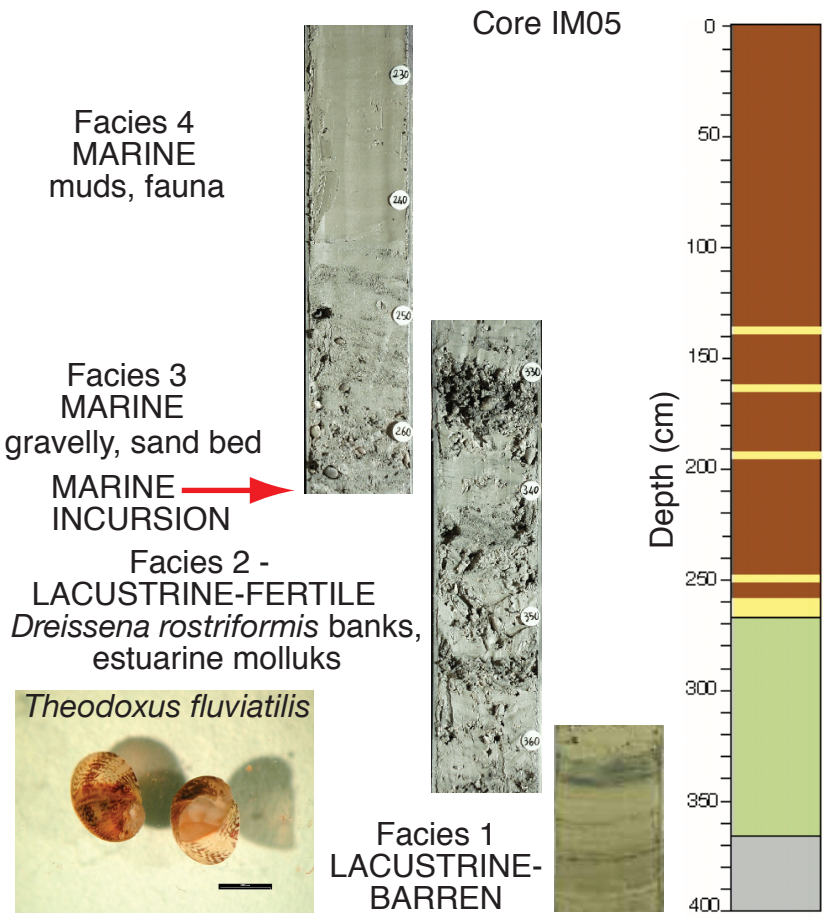
Core IM05
Facies 4
MARINE
muds, fauna
Facies 3
MARINE
gravelly, sand bed
MARINE
INCURSION
Facies 2 -
LACUSTRINE-FERTILE
Dreissena rostriformis banks,
estuarine molluks
Theodoxus fluviatilis
Facies 1
LACUSTRINE-
BARREN
Depth (cm)
0
50
100
150
200
250
300
350
400

Figure 5

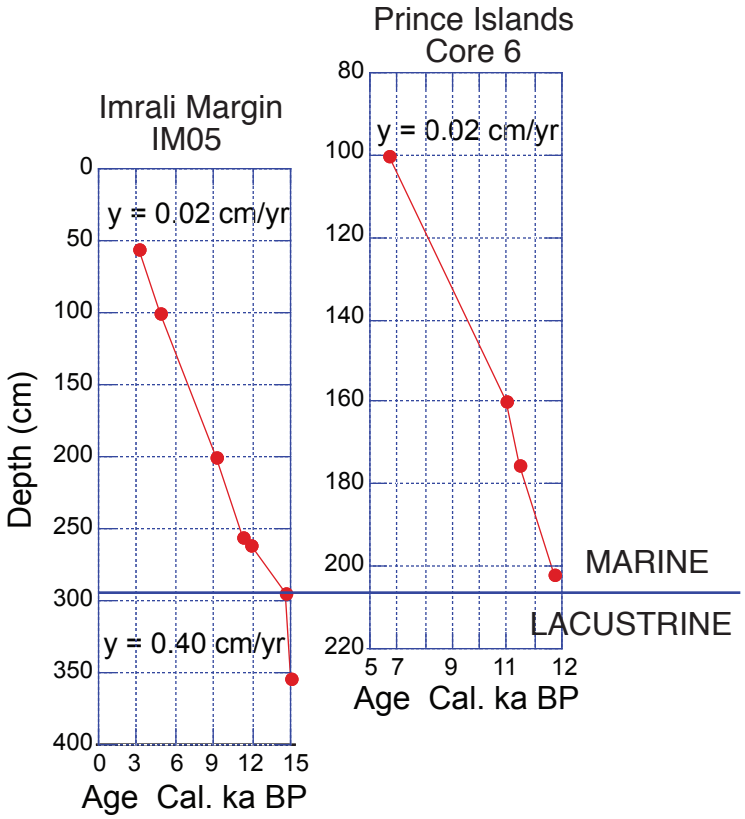
Prince Islands
Core 6
y = 0.02 cm/yr
MARINE
LACUSTRINE
Age Cal. ka BP
Imrali Margin
IM05
y = 0.02 cm/yr
y = 0.40 cm/yr
Depth (cm)
Age Cal. ka BP

Figure 6

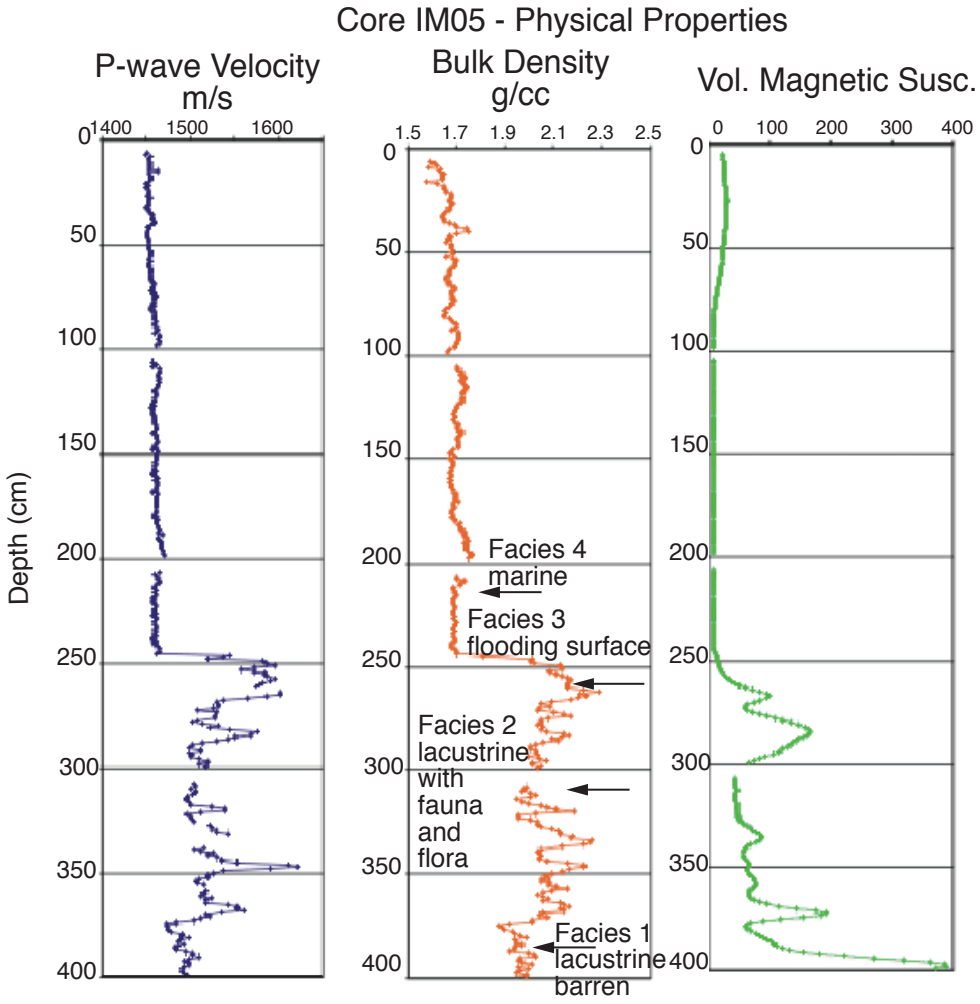
Core IM05 - Physical Properties
P-wave Velocity
m/s
1400
1500
1600
Bulk Density
g/cc
1.5
1.7
1.9
2.1
2.3
2.5
Vol. Magnetic Susc.
0
100
200
300
400
Depth (cm)
0
50
100
150
200
250
300
350
400
Facies 4
marine
Facies 3
flooding surface
Facies 2
lacustrine
with
fauna
and
flora
Facies 1
lacustrine
barren

Figure 7

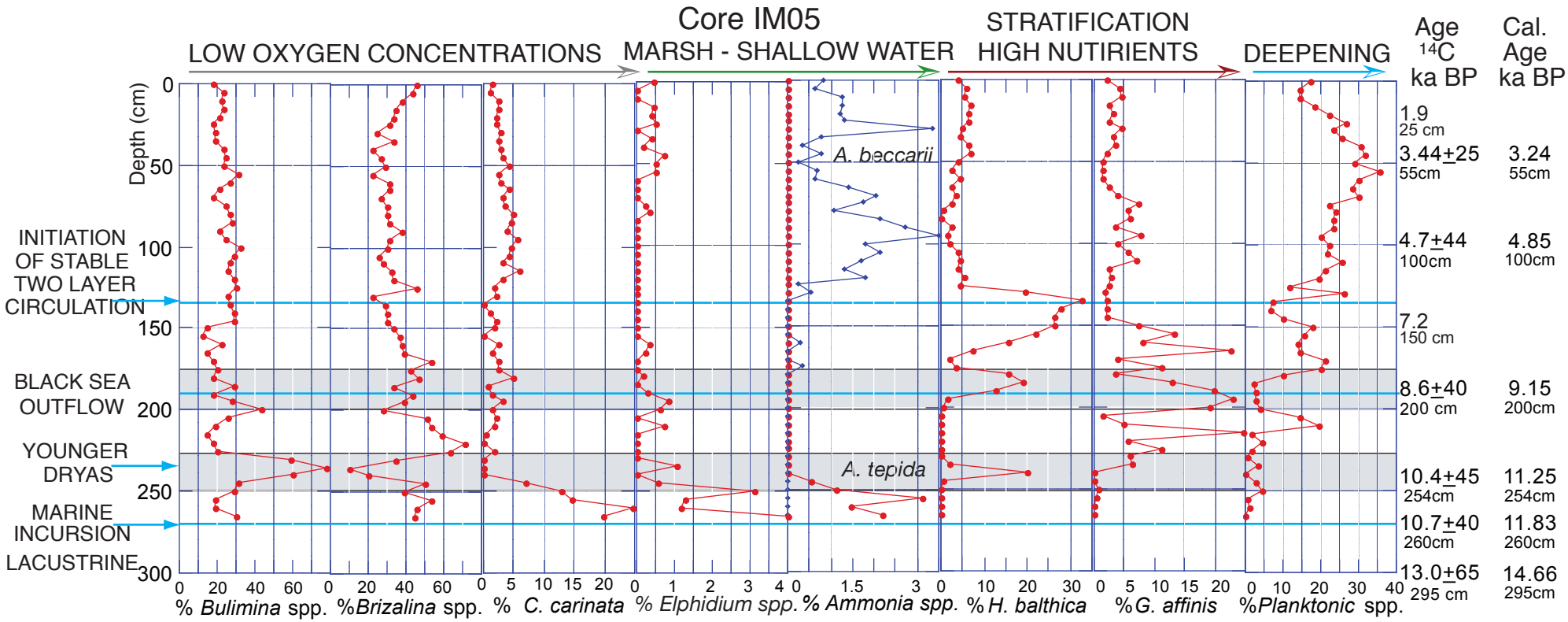
Core IM05
LOW OXYGEN CONCENTRATIONS
MARSH - SHALLOW WATER
STRATIFICATION
HIGH NUTIRIENTS
DEEPENING
Age
14C
ka BP
Cal.
Age
ka BP
Depth (cm)
INITIATION
OF STABLE
TWO LAYER
CIRCULATION
BLACK SEA
OUTFLOW
YOUNGER
DRYAS
MARINE
INCURSION
LACUSTRINE
A. beccarii
A. tepida
1.9
25 cm
3.44±25
55cm
3.24
55cm
4.7±44
100cm
4.85
100cm
7.2
150 cm
8.6±40
200 cm
9.15
200cm
10.4±45
254cm
11.25
254cm
10.7±40
260cm
11.83
260cm
13.0±65
295 cm
14.66
295cm
% Bulimina spp.
%Brizalina spp.
% C. carinata
% Elphidium spp.
% Ammonia spp.
% H. balthica
%G. affinis
%Planktonic spp.

Figure 8

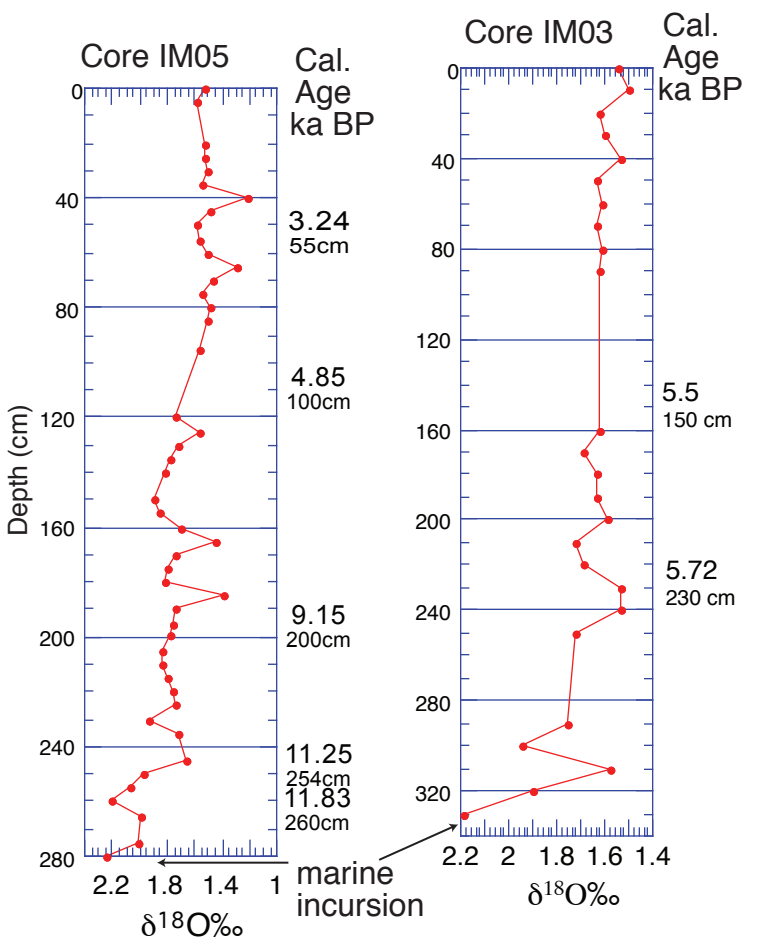
(a)
Core IM05
Cal. Age ka BP
Core IM03
Cal. Age ka BP
Depth (cm)
0
40
80
120
160
200
240
280
320
3.24
55cm
4.85
100cm
9.15
200cm
11.25
254cm
11.83
260cm
5.5
150 cm
5.72
230 cm
2.2 1.8 1.4 1
δ18O‰
marine incursion
2.2 2 1.8 1.6 1.4
δ18O‰

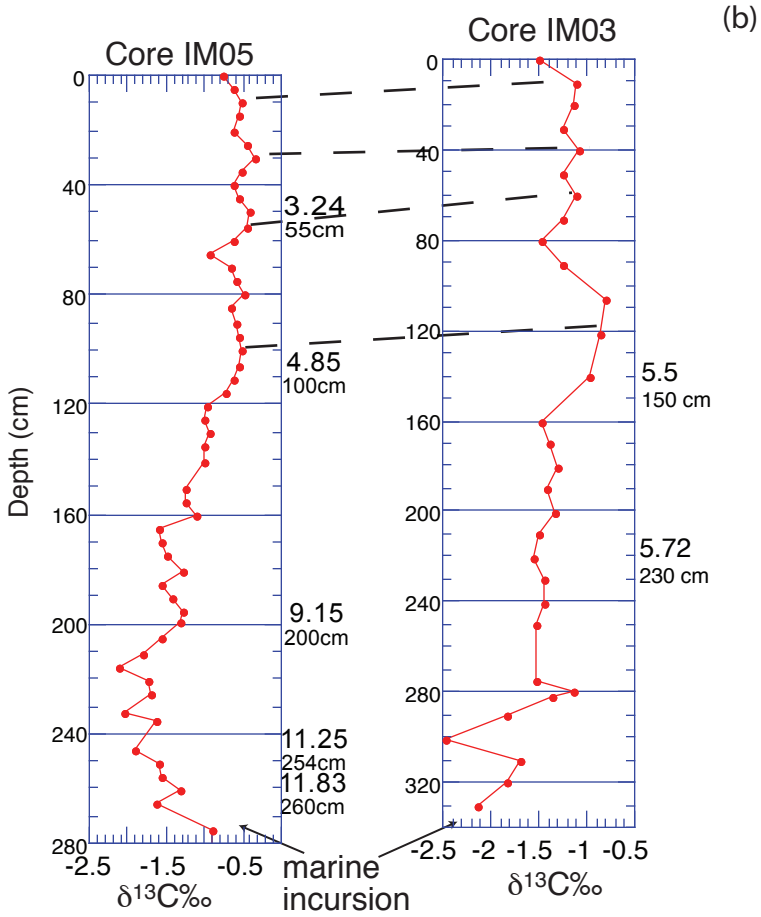
(b)
Core IM05
Core IM03
Depth (cm)
0
40
80
120
160
200
240
280
320
3.24
55cm
4.85
100cm
9.15
200cm
11.25
254cm
11.83
260cm
5.5
150 cm
5.72
230 cm
-2.5 -1.5 -0.5
δ13C‰
marine incursion
-2.5 -2 -1.5 -1 -0.5
δ13C‰

Figure 9

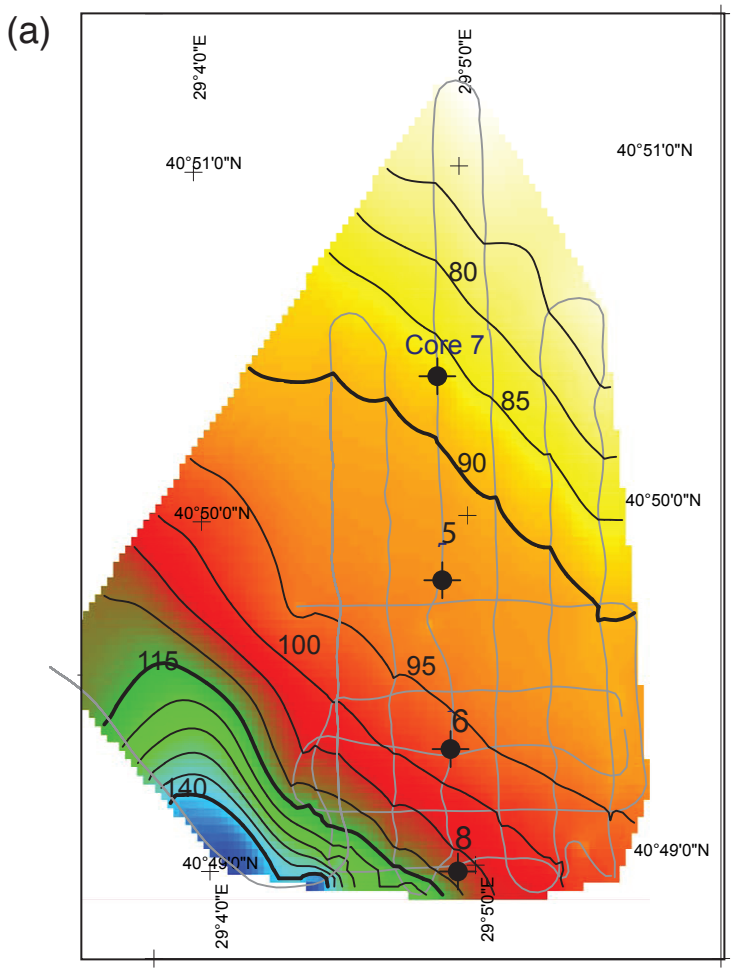
(a)
29°4'0"E
29°5'0"E
40°51'0"N
40°50'0"N
40°49'0"N
80
85
90
95
100
115
140
Core 7
5
6
8

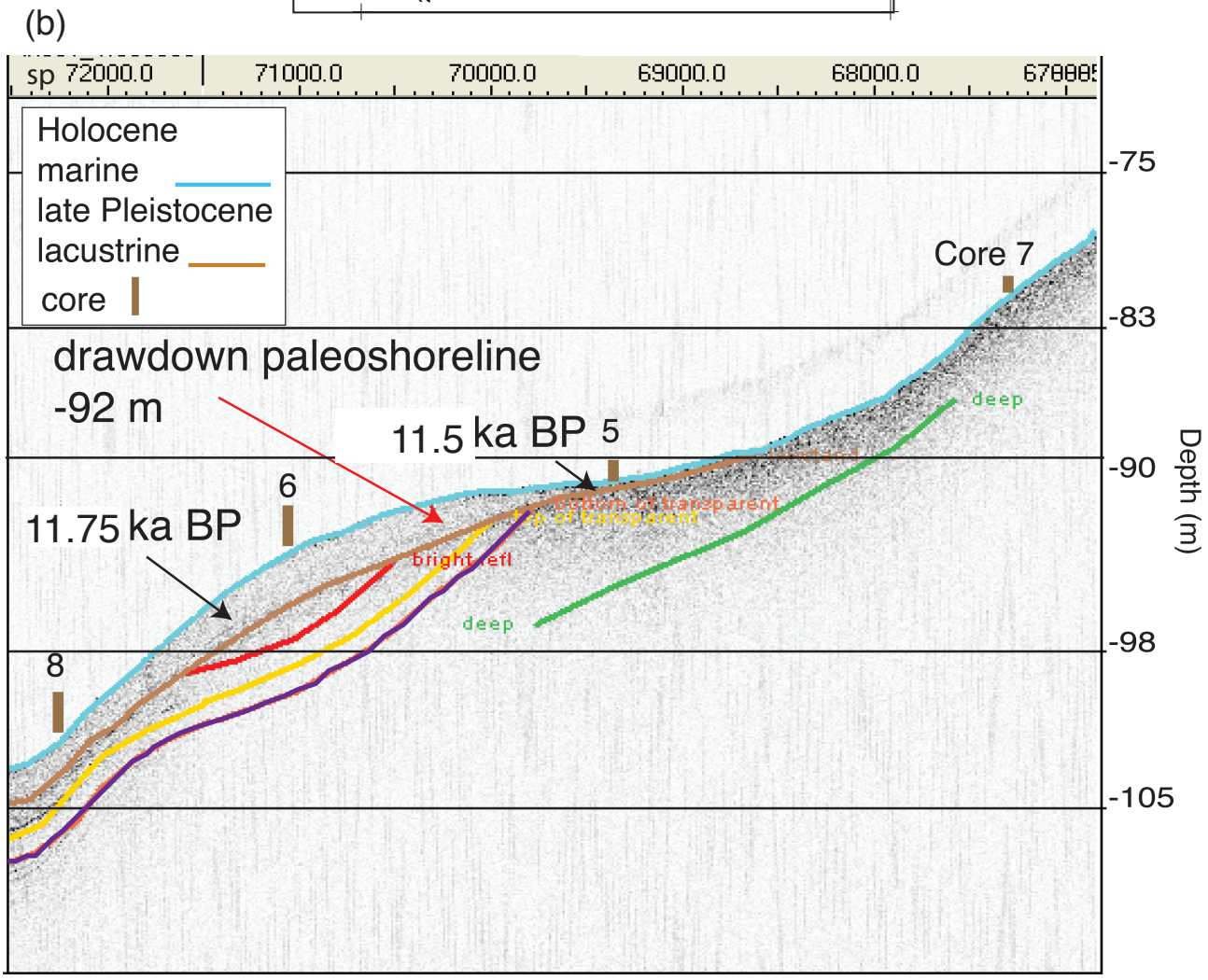
(b)
sp 72000.0
71000.0
70000.0
69000.0
68000.0
Holocene
marine
late Pleistocene
lacustrine
core
drawdown paleoshoreline
-92 m
11.5 ka BP
5
6
11.75 ka BP
8
Core 7
deep
bright refl
deep
-75
-83
-90
-98
-105
Depth (m)

Figure 10.

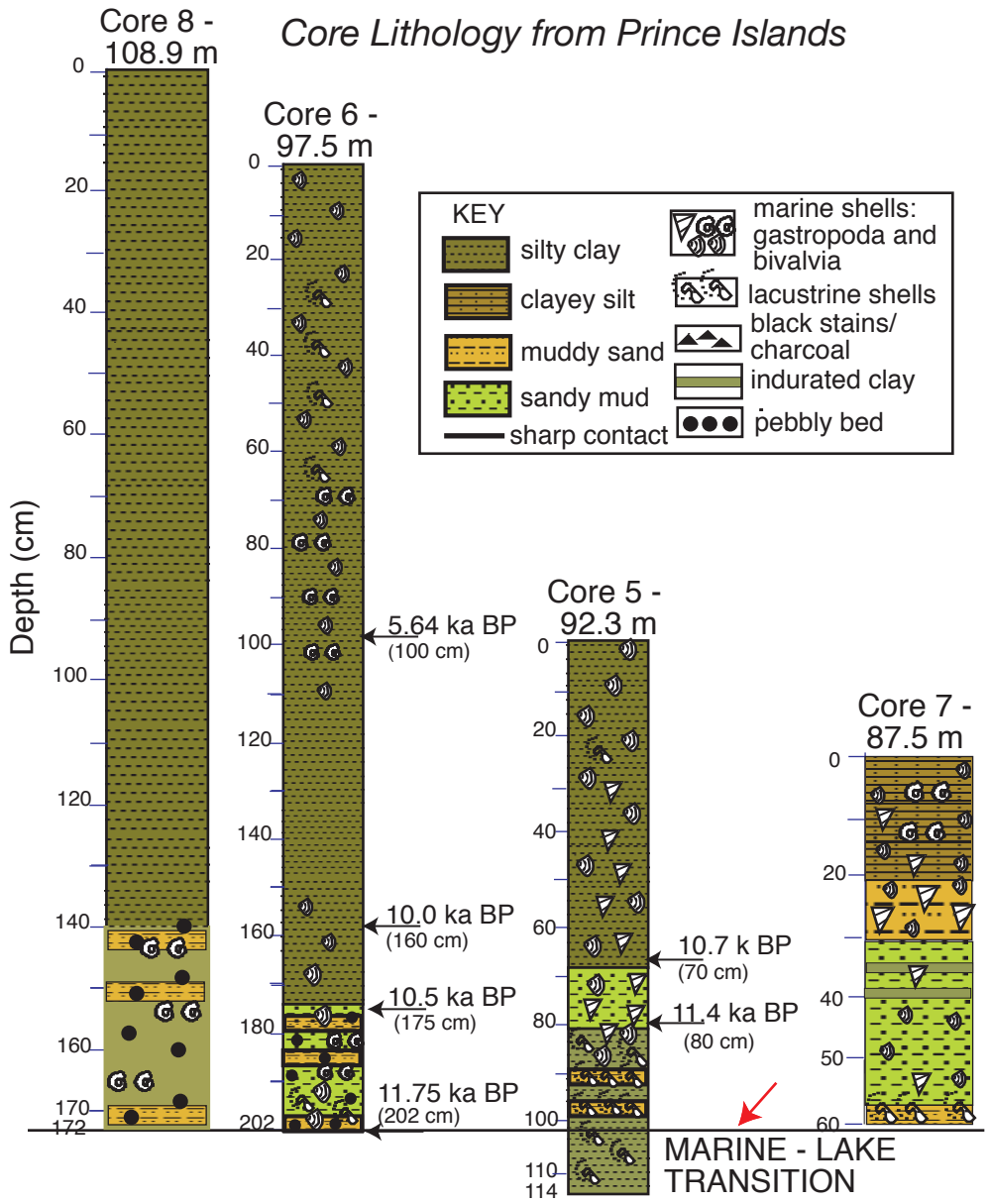
Core Lithology from Prince Islands
Core 8 - 108.9 m
Core 6 - 97.5 m
Core 5 - 92.3 m
Core 7 - 87.5 m
Depth (cm)
KEY
silty clay
clayey silt
muddy sand
sandy mud
sharp contact
marine shells: gastropoda and bivalvia
lacustrine shells
black stains/ charcoal
indurated clay
pebbly bed
5.64 ka BP (100 cm)
10.0 ka BP (160 cm)
10.5 ka BP (175 cm)
11.75 ka BP (202 cm)
10.7 k BP (70 cm)
11.4 ka BP (80 cm)
MARINE - LAKE TRANSITION

Figure 11

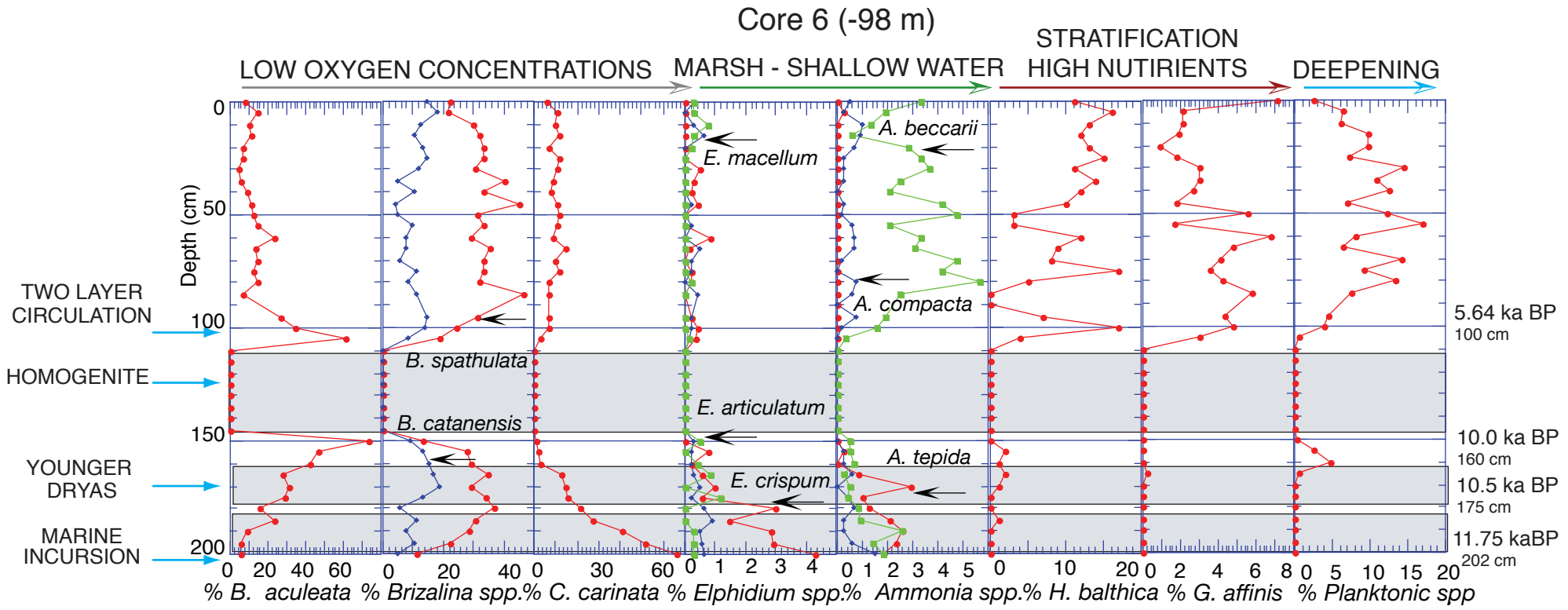
Core 6 (-98 m)
LOW OXYGEN CONCENTRATIONS
MARSH - SHALLOW WATER
STRATIFICATION
HIGH NUTIRIENTS
DEEPENING
Depth (cm)
0
50
100
150
200
TWO LAYER CIRCULATION
HOMOGENITE
YOUNGER DRYAS
MARINE INCURSION
A. beccarii
E. macellum
A. compacta
B. spathulata
B. catanensis
E. articulatum
A. tepida
E. crispum
5.64 ka BP
100 cm
10.0 ka BP
160 cm
10.5 ka BP
175 cm
11.75 kaBP
202 cm
0 20 40 60
0 20 40
0 30 60
0 1 2 3 4
0 1 2 3 4 5
0 10 20
0 2 4 6 8
0 5 10 15 20
% B. aculeata
% Brizalina spp.
% C. carinata
% Elphidium spp.
% Ammonia spp.
% H. balthica
% G. affinis
% Planktonic spp

Figure 12

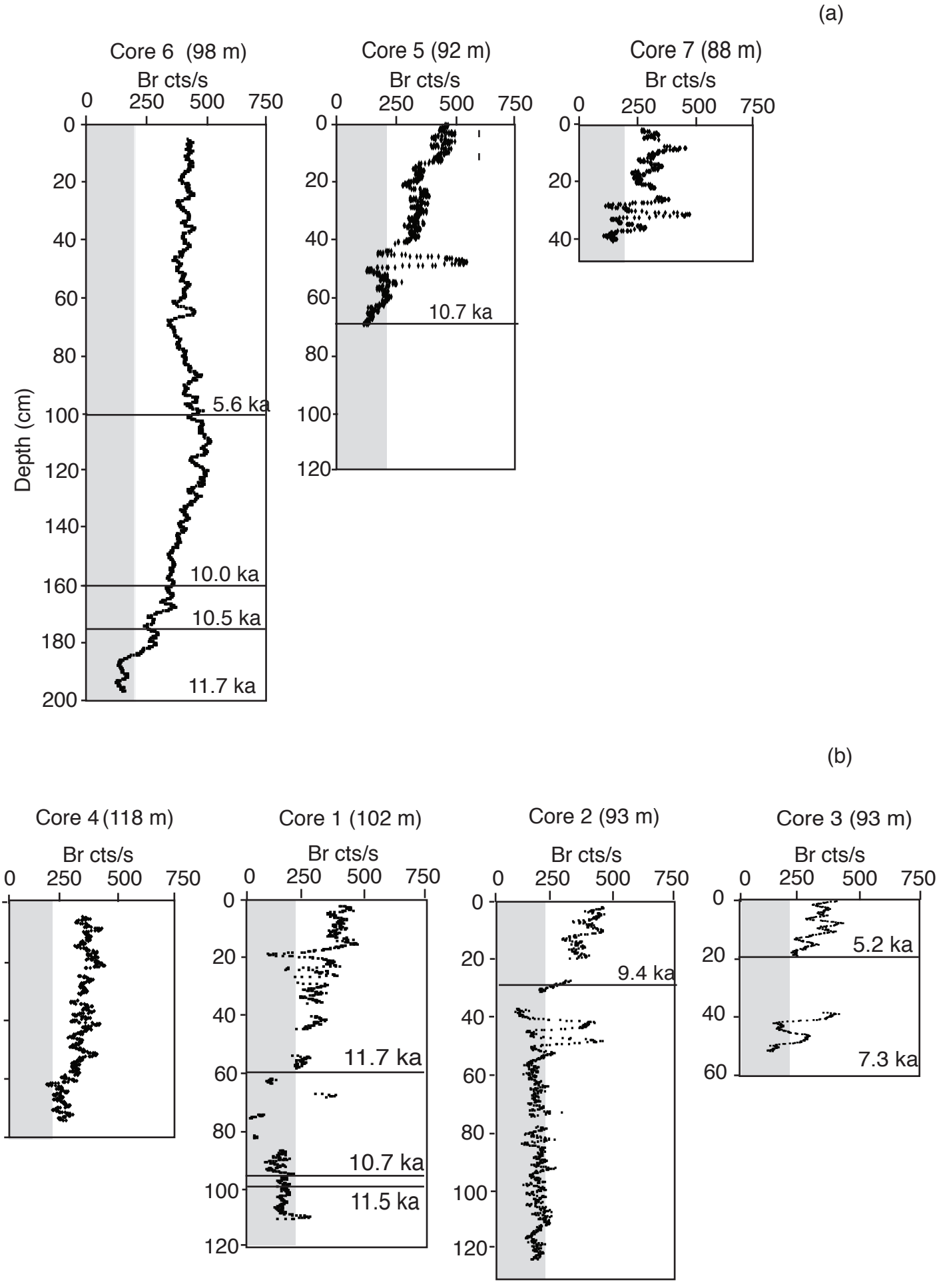
(a)
Core 6 (98 m)
Core 5 (92 m)
Core 7 (88 m)
Br cts/s
0 250 500 750
Depth (cm)
5.6 ka
10.7 ka
10.0 ka
10.5 ka
11.7 ka
(b)
Core 4 (118 m)
Core 1 (102 m)
Core 2 (93 m)
Core 3 (93 m)
11.7 ka
10.7 ka
11.5 ka
9.4 ka
5.2 ka
7.3 ka

Figure 13

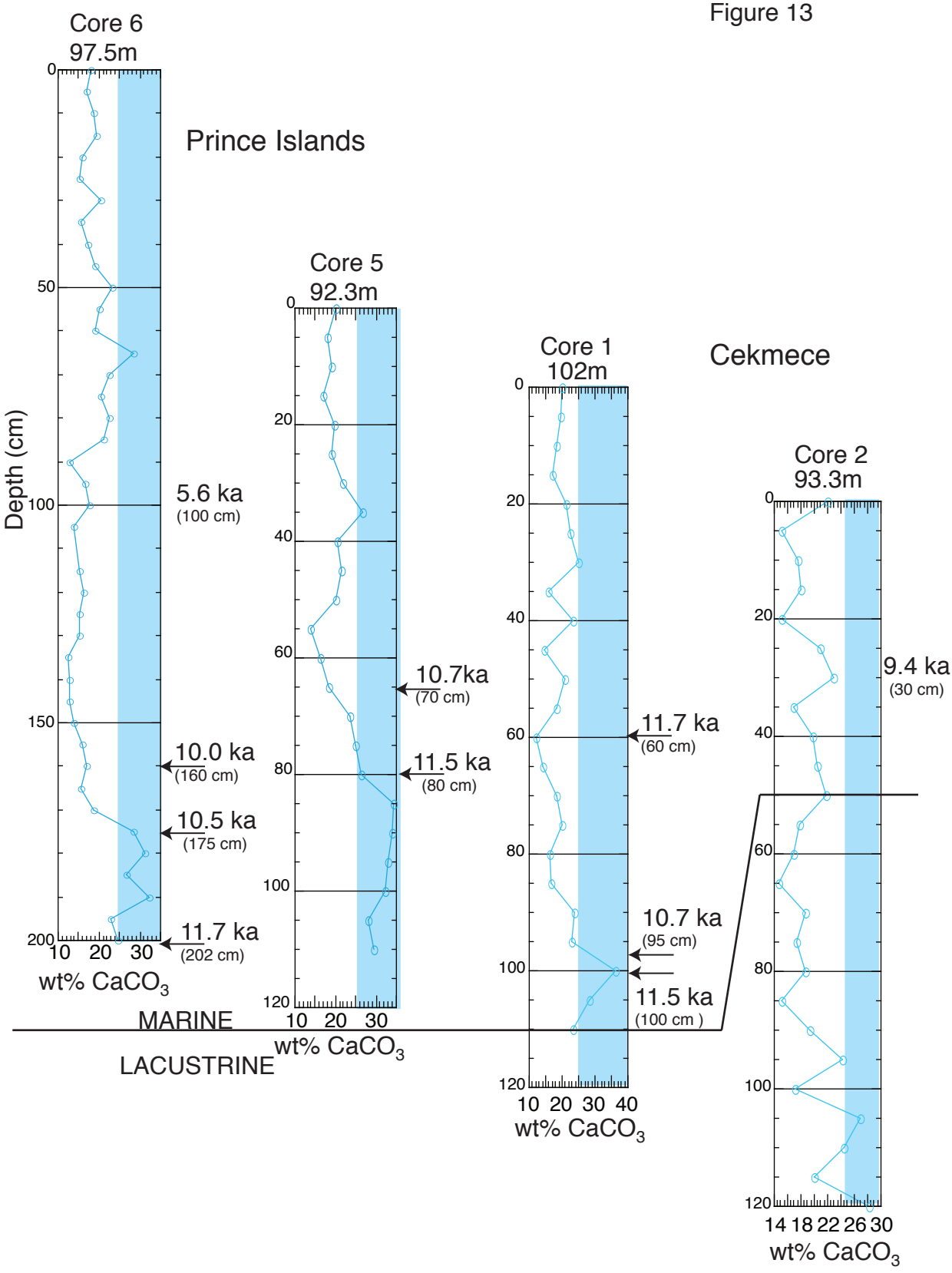
Core 6
97.5m
Prince Islands
Core 5
92.3m
Core 1
102m
Cekmece
Core 2
93.3m
Depth (cm)
0
50
100
150
200
5.6 ka
(100 cm)
10.0 ka
(160 cm)
10.5 ka
(175 cm)
11.7 ka
(202 cm)
10 20 30
wt% CaCO3
0
20
40
60
80
100
120
10.7ka
(70 cm)
11.5 ka
(80 cm)
10 20 30
wt% CaCO3
0
20
40
60
80
100
120
11.7 ka
(60 cm)
10.7 ka
(95 cm)
11.5 ka
(100 cm)
10 20 30 40
wt% CaCO3
0
20
40
60
80
100
120
9.4 ka
(30 cm)
14 18 22 26 30
wt% CaCO3
MARINE
LACUSTRINE

Figure 14

(a)

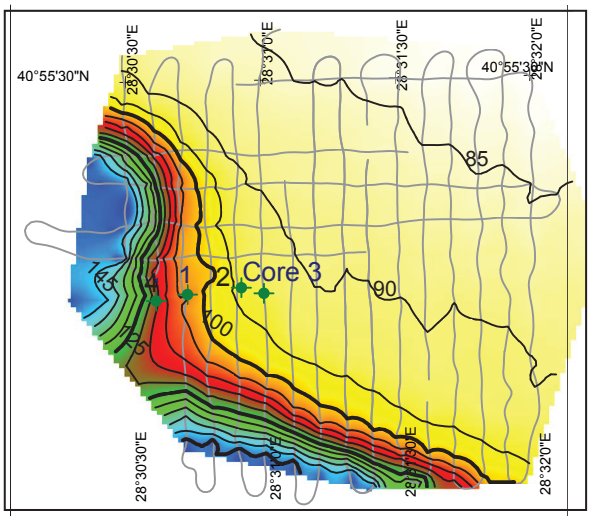
40°55'30"N
28°30'30"E
28°37'0"E
28°31'30"E
28°32'0"E
85
90
95
100
105
Core 3
1
2
4

(b)

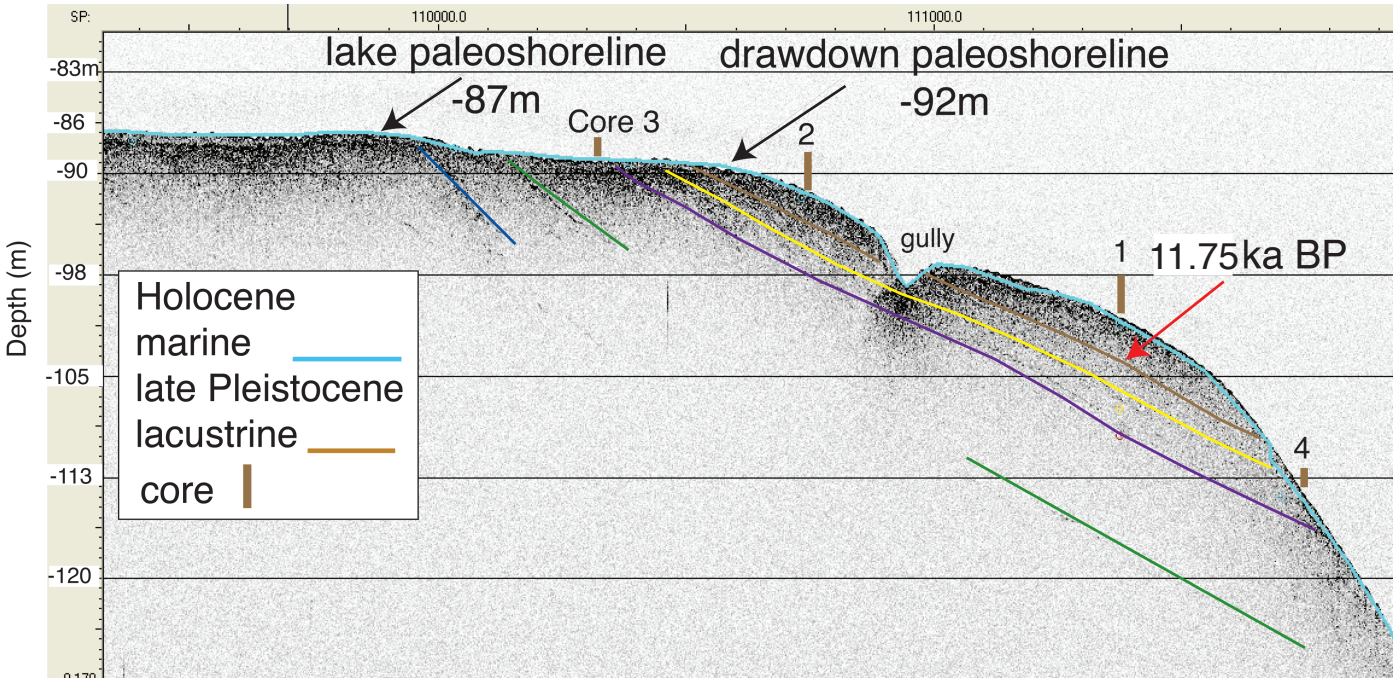
SP:
110000.0
111000.0
lake paleoshoreline
-87m
drawdown paleoshoreline
-92m
Core 3
2
gully
1
11.75ka BP
4
Holocene marine
late Pleistocene lacustrine
core
Depth (m)
-83m
-86
-90
-98
-105
-113
-120

Figure 15

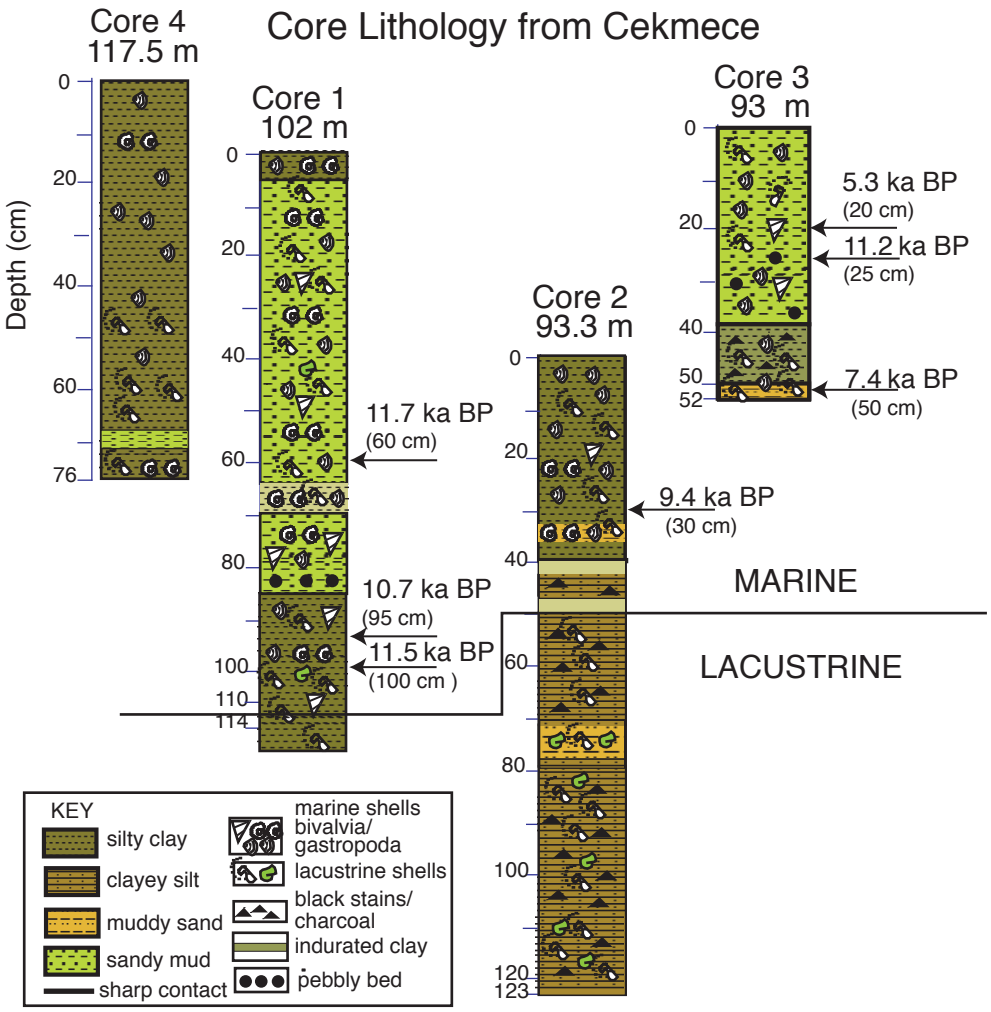
Core Lithology from Cekmece
Core 4
117.5 m
Core 1
102 m
Core 3
93 m
Core 2
93.3 m
Depth (cm)
0
20
40
60
76
80
100
110
114
52
50
120
123
11.7 ka BP
(60 cm)
10.7 ka BP
(95 cm)
11.5 ka BP
(100 cm)
5.3 ka BP
(20 cm)
11.2 ka BP
(25 cm)
7.4 ka BP
(50 cm)
9.4 ka BP
(30 cm)
MARINE
LACUSTRINE
KEY
silty clay
clayey silt
muddy sand
sandy mud
sharp contact
marine shells bivalvia/ gastropoda
lacustrine shells
black stains/ charcoal
indurated clay
pebbly bed

Figure 16

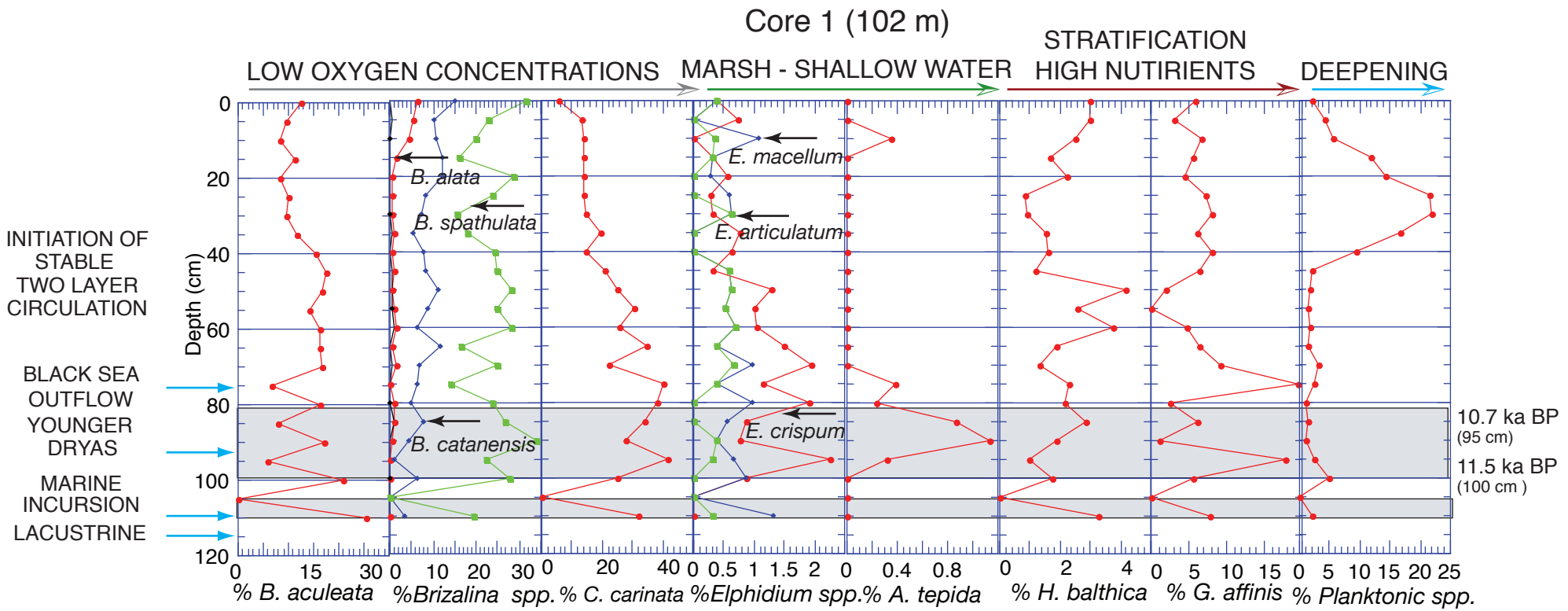
Core 1 (102 m)
LOW OXYGEN CONCENTRATIONS
MARSH - SHALLOW WATER
STRATIFICATION
HIGH NUTIRIENTS
DEEPENING
INITIATION OF STABLE TWO LAYER CIRCULATION
BLACK SEA OUTFLOW
YOUNGER DRYAS
MARINE INCURSION
LACUSTRINE
Depth (cm)
B. alata
B. spathulata
B. catanensis
E. macellum
E. articulatum
E. crispum
10.7 ka BP
(95 cm)
11.5 ka BP
(100 cm)
% B. aculeata
%Brizalina spp.
% C. carinata
%Elphidium spp.
% A. tepida
% H. balthica
% G. affinis
% Planktonic spp.

Figure 17

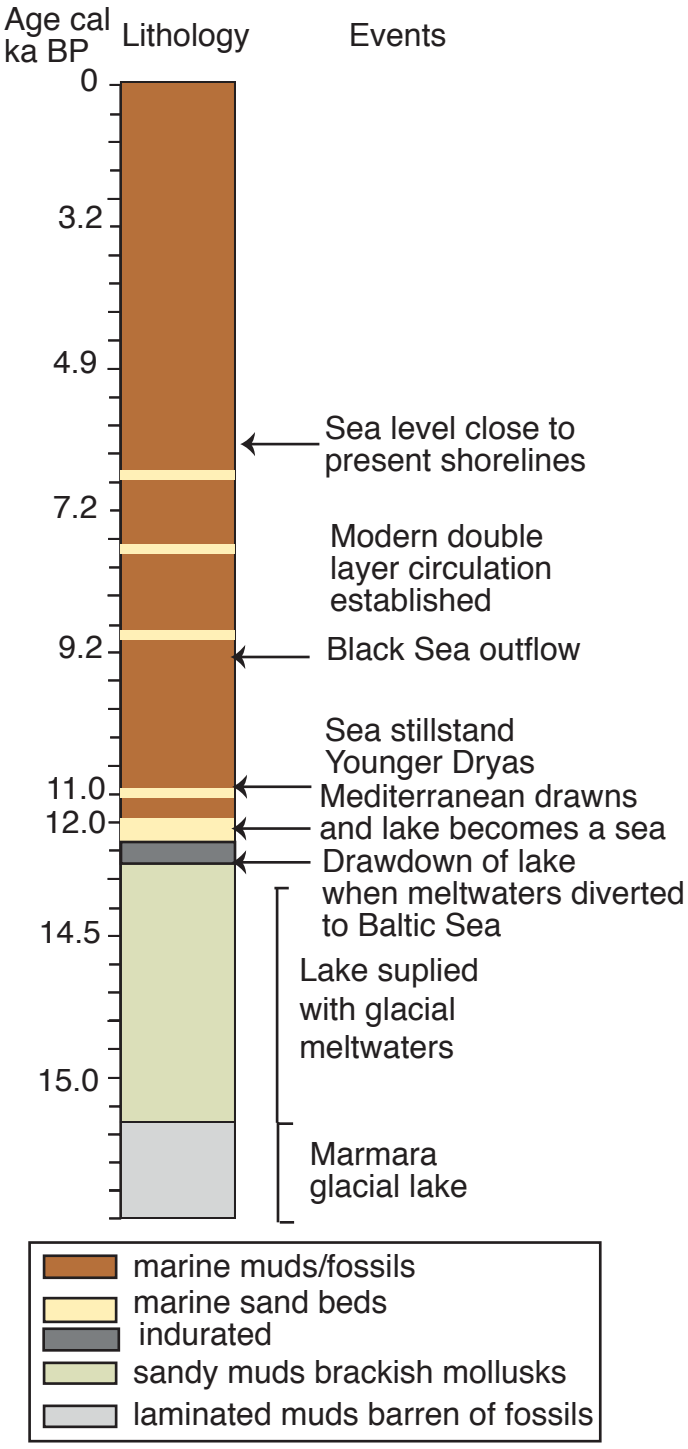
Age cal ka BP
Lithology
Events
0
3.2
4.9
7.2
9.2
11.0
12.0
14.5
15.0
Sea level close to present shorelines
Modern double layer circulation established
Black Sea outflow
Sea stillstand Younger Dryas
Mediterranean drawns and lake becomes a sea
Drawdown of lake when meltwaters diverted to Baltic Sea
Lake suplied with glacial meltwaters
Marmara glacial lake
marine muds/fossils
marine sand beds
indurated
sandy muds brackish mollusks
laminated muds barren of fossils